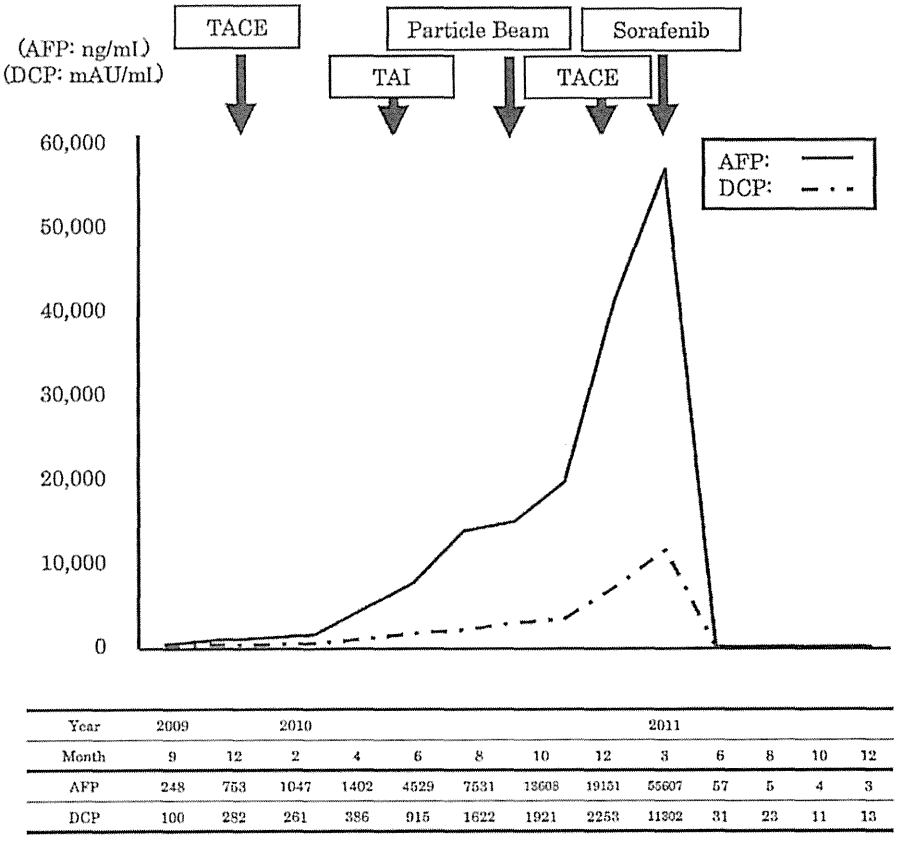

Year	2009		2010						2011				
Month	9	12	2	4	6	8	10	12	3	6	8	10	12
AFP	248	753	1047	1402	4529	7531	13608	19151	55607	57	5	4	3
DCP	100	282	261	386	915	1622	1921	2253	11302	31	23	11	13

Figure 2. Changes in the levels of alpha-fetoprotein (AFP) and des-gamma-carboxy prothrombin (DCP) over the past two years.

Table. CR in HCC Patients Receiving Sorafenib Treatment

Author	Gender	Age	Etiology	Distant Metastasis	Time to cessation	Time to CR
Hagihara	M	65	HCV	Lung	21 days	unknown
Inuzuka[16]	F	76	HCV	Lung	4 months	3 months
So[8]	M	78	Hemo-chromatosis	Lung	6 months	5 months
Curtit[13]	M	56	HCV	No	6 months	6 months
Irtan[15]	M	59	Hemo-chromatosis	Lymph node, Omentum	6 months	6 months
Wang[10]	M	74	HCV	No	8 months	8 months
Kudo[11]	M	68	HBV	Lung	none	2 months
Chelis[12]	M	69	HBV, HIV	Lymph node	none	6 months
Sacco[14]	M	84	HCV	No	none	6 months
Yeganeh[9]	M	54	HBV	Lung	none	18 months

biomarkers. There are some successful examples, as is the case with erlotinib/gefitinib in lung cancer patients with the epidermal growth factor receptor (EGFR) mutation (21), trastuzumab in breast cancer patients with HER2 amplification (22), cetuximab in colorectal cancer patients with the K-ras wild-type expression (23) and so on. Unfortunately, with respect to hepatocellular carcinoma, no biomarkers predicting the response to sorafenib have been identified in large-scale studies (24). This is due to the heterogeneity of hepatocellular carcinoma (25, 26). In some particular situations, such as in patients with a small tumor burden, favorable outcomes may be achieved, in which tumors are accidentally sensitive to sorafenib. The drug sensitivity profile may change if there exists a certain genetic polymorphism or certain interactions with other drugs. The plasma concentration of sorafenib in this patient was different for an unknown reason. The Barcelona-Clinic Liver Cancer staging classification and treatment schedule proposed by the American Association for the Study of Liver Disease recommend that the treatment method for hepatocellular carcinoma be determined based on the progression of hepatocellular carcinoma, the liver function and the performance status. Although pulmonary metastasis existed in this case, the HCC in the patient's liver and inferior vena cava were almost controlled with TACE, transcatheter arterial infusion chemotherapy (TAI) and particle beam radiation therapy, and the number of tumors was reduced. Before administering sorafenib medication, every effort should be made to reduce the number of tumors. It is also very important to improve the liver function, which affects the applicability of treatment. If tumors in the liver are controlled and the liver function is improved, it is worth prescribing sorafenib in patients for only a short time. The immune system plays a role in tumor regression. Vascular endothelial growth factor (VEGF) inhibits the differentiation and maturation of dendritic cells and thus plays a potential immunosuppressive role (27). Sorafenib targets VEGF-mediated angiogenesis (5), which suggests the role of sorafenib in upregulating the immune system (28). Immunological factors may play an important role in this rare phenomenon; however, to date, this role remains

incompletely understood (29).

Conclusion

We experienced a rare case of a complete response following short-term treatment with sorafenib in a patient with advanced HCC with lung metastasis. Further studies are required to elucidate the precise mechanisms of this phenomenon. It is important to accumulate and carefully analyze these rare cases in order to explore the development of new therapies for advanced HCC.

The authors state that they have no Conflict of Interest (COI).

Acknowledgement

We thank the office administrators for their support (Ms. Chie Setagawa and Mayu Ohira).

Funding

This study was supported by a Grant-in-Aid for Cancer Research from the Ministry of Health, Labour and Welfare, Japan.

References

1. Jemal A, Bray F, Center MM, et al. Global cancer statistics. CA Cancer J Clin **61**: 69-90, 2011.
2. Llovet JM, Burroughs A, Bruix J. Hepatocellular carcinoma. Lancet **362**: 1907-1917, 2003.
3. Llovet JM, Di Bisceglie AM, Bruix J, et al. Design and endpoints of clinical trials in hepatocellular carcinoma. J Natl Cancer Inst **100**: 698-711, 2008.
4. Bruix J, Sherman M. Management of hepatocellular carcinoma: an update. Hepatology **53**: 1020-1022, 2011.
5. Wilhelm SM, Carter C, Tang L, et al. BAY 43-9006 exhibits broad spectrum oral antitumor activity and targets the RAF/MEK/ERK pathway and receptor tyrosine kinases involved in tumor progression and angiogenesis. Cancer Res **64**: 7099-7109, 2004.
6. Llovet JM, Ricci S, Mazzaferro V, et al. Sorafenib in advanced hepatocellular carcinoma. N Engl J Med **359**: 378-390, 2008.
7. Cheng AL, Kang YK, Chen Z, et al. Efficacy and safety of sorafenib in patients in the Asia-Pacific region with advanced hepatocellular carcinoma: a phase III randomised, double-blind, placebo-controlled trial. Lancet Oncol **10**: 25-34, 2009.
8. So BJ, Bekaii-Saab T, Bloomston MA, et al. Complete clinical response of metastatic hepatocellular carcinoma to sorafenib in a patient with hemochromatosis: a case report. J Hematol Oncol **1**: 18, 2008.
9. Yeganeh M, Finn RS, Saab S. Apparent remission of a solitary metastatic pulmonary lesion in a liver transplant recipient treated with sorafenib. Am J Transplant **9**: 2851-2854, 2009.
10. Wang SX, Byrnes A, Verma S, et al. Complete remission of unresectable hepatocellular carcinoma treated with reduced dose of sorafenib: a case report. Target Oncol **5**: 59-63, 2010.
11. Kudo M, Ueshima K. Positioning of a molecular-targeted agent, sorafenib, in the treatment algorithm for hepatocellular carcinoma and implication of many complete remission cases in Japan. Oncology **78** Suppl 1: 154-166, 2010.
12. Chelis L, Ntinos N, Souftas V, et al. Complete response after sorafenib therapy for hepatocellular carcinoma in an HIV-HBV co infected patient: Possible synergy with HAART? A case report. Med Oncol **28** Suppl 1: 165-168, 2010.
13. Curtit E, Thiery-Vuillemin A, Nguyen T, et al. Complete histologic response induced by sorafenib in advanced hepatocellular carcinoma: a case report. J Clin Oncol **29**: e330-e332, 2011.
14. Sacco R, Bargellini I, Gianluigi G, et al. Complete response for advanced liver cancer during sorafenib therapy: case report. BMC Gastroenterol **11**: 4, 2011.
15. Irtan S, Chopin-Laly X, Ronot M, et al. Complete regression of locally advanced hepatocellular carcinoma induced by sorafenib allowing curative resection. Liver Int **31**: 740-743, 2011.
16. Inuzuka T, Nishikawa H, Sekikawa A, et al. Complete response of advanced hepatocellular carcinoma with multiple lung metastases treated with sorafenib: a case report. Oncology **81** Suppl 1: 152-157, 2011.
17. Cole WH, Everson TC. Spontaneous regression of cancer: preliminary report. Ann Surg **144**: 366-383, 1956.
18. Cole WH. Relationship of causative factors in spontaneous regression of cancer to immunologic factors possibly effective in cancer. J Surg Oncol **8**: 391-411, 1976.
19. Cole WH. Efforts to explain spontaneous regression of cancer. J Surg Oncol **17**: 201-209, 1981.
20. Lathia C, Lettieri J, Cihon F, et al. Lack of effect of ketoconazole-mediated CYP3A inhibition on sorafenib clinical pharmacokinetics. Cancer Chemother Pharmacol **57**: 685-692, 2006.
21. Cohen MH, Williams GA, Sridhara R, et al. FDA drug approval summary: gefitinib (ZD1839) (Iressa) tablets. Oncologist **8**: 303-306, 2003.
22. Slamon DJ, Leyland-Jones B, Shak S, et al. Use of chemotherapy plus a monoclonal antibody against HER2 for metastatic breast cancer that overexpresses HER2. N Engl J Med **344**: 783-792, 2001.
23. Karapetis CS, Khambata-Ford S, Jonker DJ, et al. K-ras mutations and benefit from cetuximab in advanced colorectal cancer. N Engl J Med **359**: 1757-1765, 2008.
24. Llovet JM, Pena CE, Lathia CD, et al. Plasma biomarkers as predictors of outcome in patients with advanced hepatocellular carcinoma. Clin Cancer Res **18**: 2290-2300, 2012.
25. Villanueva A, Llovet JM. Targeted therapies for hepatocellular carcinoma. Gastroenterology **140**: 1410-1426, 2011.
26. Villanueva A, Llovet JM. Impact of intra-individual molecular heterogeneity in personalized treatment of hepatocellular carcinoma. Hepatology **56**: 2416-2419, 2012.
27. Alfaro C, Suarez N, Gonzalez A, et al. Influence of bevacizumab, sunitinib and sorafenib as single agents or in combination on the inhibitory effects of VEGF on human dendritic cell differentiation from monocytes. Br J Cancer **100**: 1111-1119, 2009.
28. Cao M, Xu Y, Youn JI, et al. Kinase inhibitor Sorafenib modulates immunosuppressive cell populations in a murine liver cancer model. Lab Invest **91**: 598-608, 2011.
29. Kondo S, Okusaka T, Ueno H, et al. Spontaneous regression of hepatocellular carcinoma. Int J Clin Oncol **11**: 407-411, 2006.

Oncogene (2004) 23, 8705–8710

www.nature.com/onc

Identification of 27 5′ CpG islands aberrantly methylated and 13 genes silenced in human pancreatic cancers

Atsushi Hagihara[1,2,3], Kazuaki Miyamoto[1], Junichi Furuta[1], Nobuyoshi Hiraoka[4], Kuniko Wakazono[1], Shuichi Seki[3], Shoji Fukushima[2], Ming-Sound Tsao[5], Takashi Sugimura[1] and Toshikazu Ushijima[1,*]

[1]*Carcinogenesis Division, National Cancer Center Research Institute, 1-1 Tsukiji 5-chome, Chuo-ku, Tokyo 104-0045, Japan;* [2]*Department of Pathology, Osaka City University Graduate School of Medicine, 1-4-3 Asahi-machi, Abeno-ku, Osaka 545-8585, Japan;* [3]*Department of Internal Medicine, Osaka City University Graduate School of Medicine, 1-4-3 Asahi-machi, Abeno-ku, Osaka 545-8585, Japan;* [4]*Pathology Division, National Cancer Center Research Institute, 1-1 Tsukiji 5-chome, Chuo-ku, Tokyo 104-0045, Japan;* [5]*Department of Medical Biophysics, University of Toronto, 610 University Avenue, Toronto, Ontario, Canada M5G 2M9*

Aberrantly methylated DNA fragments were searched for in human pancreatic cancers, using the genome scanning technique: methylation-sensitive-representational difference analysis (MS-RDA). MS-RDA isolated 111 DNA fragments derived from CpG islands (CGIs), and 35 of them were from CGIs in the 5′ regions of known genes. Methylation-specific PCR (MSP) of the CGIs in seven pancreatic cancer cell lines and two pancreatic ductal epithelial cell lines showed that 27 CGIs in the 5′ regions were aberrantly methylated in at least one of the cancer cell lines. Quantitative reverse-transcription–PCR analysis showed that downstream genes of all the CGIs were either not expressed or only very weakly expressed in cancer cell lines with the aberrant methylation. In the pancreatic ductal epithelial cell lines, 18 genes were expressed at various levels, and nine genes were not expressed at all. Treatment of a cancer cell line with a demethylating agent, 5-aza-2′-deoxycytidine, restored the expression of 13 genes, *RASGRF2*, *ADAM23*, *NEF3*, *NKX2-8*, *HAND1*, *EGR4*, *PRG2*, *FBN2*, *CDH2*, *TLL1*, *NPTX1*, *NTSR1* and *THBD*, showing their silencing by methylation of their 5′ CGIs. MSP of 24 primary pancreatic cancers showed that all these genes, except for *THBD*, were methylated in at least one cancer. Some of those were suggested to be potentially involved in pancreatic cancer development and progression.
Oncogene (2004) **23,** 8705–8710. doi:10.1038/sj.onc.1207783
Published online 27 September 2004

Keywords: methylation; pancreatic cancer; CpG island; silencing

Pancreatic cancer is one of the most refractory neoplasms, with the average 5-year survival being less than 20% (Jemal *et al.*, 2003). In addition to the anatomical location of the pancreas that makes early detection of pancreatic cancers very difficult, several genetic and biological characteristics, such as the presence of severe chromosomal instability and the strong involvement of stromal tissues, are considered to underlie their poor prognosis (Bardeesy and DePinho, 2002). As genetic alterations in pancreatic cancers, mutational activation of K-*ras* (90%) (Almoguera *et al.*, 1988) and inactivation of *p16* (80%), *p53* (50–70%), and *SMAD4/DPC4* (50%) by mutations and allelic losses (Caldas *et al.*, 1994; Hahn *et al.*, 1996; Rozenblum *et al.*, 1997; Wilentz *et al.*, 2000) are well-known.

Epigenetic alterations are also known to be involved in pancreatic cancers, including inactivation of *p16*, *RARβ* and *TIMP-3* by methylation of promoter CpG islands (CGIs) (Herman *et al.*, 1995; Merlo *et al.*, 1995; Ueki *et al.*, 2000). Considering that multiple tumor-suppressor genes are inactivated by methylation in human pancreatic cancers, genome-wide scanning for genes that are inactivated by methylation of promoter CGIs is important. By methylated CpG island amplification/representational difference analysis (MCA/RDA) technique (Toyota *et al.*, 1999), Ueki *et al.* (2001) identified seven CGIs differentially methylated in pancreatic cancers. By cDNA microarray analysis of genes whose expressions were induced by a demethylating agent, 5-aza-2′-deoxycytidine (5-aza-dC), Sato *et al.* (2003) identified 11 genes whose promoter CGIs were aberrantly methylated.

In a genome-scanning technique, methylation-sensitive-RDA (MS-RDA) (Ushijima *et al.*, 1997), unmethylated, CpG-rich regions of the genome can be amplified from two genomes using methylation-sensitive restriction enzymes, such as *Hpa*II, *Sac*II, and *Nar*I, and the two 'amplicons' are compared by RDA (Lisitsyn and Wigler, 1993). By this strategy, diverse CpG islands in the genome can be scanned (Kaneda *et al.*, 2003), and genes silenced in human stomach, breast and lung cancers have been identified (Takai *et al.*, 2001; Kaneda *et al.*, 2002; Asada *et al.*, 2003; Miyamoto *et al.*, 2003). In this study, MS-RDA was applied to human pancreatic cancers.

*Correspondence: T Ushijima; E-mail: tushijim@ncc.go.jp
Received 4 December 2003; revised 10 March 2004; accepted 1 April 2004; published online 27 September 2004

Isolation of differentially methylated DNA fragments by MS-RDA

DNA fragments methylated in a pancreatic cancer cell line, HPAC, but not in an immortalized human pancreatic ductal epithelial cell line, HPDE-4/E6E7 (Furukawa *et al.*, 1996; Liu *et al.*, 1998), were searched for by three series of MS-RDA, using *Hpa*II, *Sac*II and *Nar*I. A total of 295 DNA fragments were obtained in the three series. By sequencing them using ABI PRISM310 (PE Biosystems, Foster City, CA, USA), 168 DNA fragments were found to be nonredundant. By BLAST search at a GenBank web site, 111 DNA fragments of them were found to be derived from CGIs, and 40 were derived from CGIs in the 5′ regions of genes (Table 1). We selected CGIs that met a criterion described by D Takai and PA Jones (Takai and Jones, 2002).

From the 40 CGIs in the 5′ regions of genes, 35 CGIs located in the 5′ regions of known genes were selected. Their methylation statuses were examined by methylation-specific PCR (MSP) (primer sequences in Supplementary Table 1) using two immortalized human pancreatic ductal epithelial cell lines (HPDE-4/E6E7 and HPDE6-E6E7c7) and seven pancreatic cancer cell lines (American Type Culture Collection, Rockville, MD, USA). CGIs in the 5′ regions of 27 genes (Figure 1), *RASGRF2*, *ADAM23*, *NEF3*, *OLIG3*, *FGF14*, *NKX2-8*, *SALPR*, *RAX*, *RGS17*, *NGN1*, *HAND1*, *SOX5*, *RGS20*, *EGR4*, *ADAMTS19*, *PRG2*, *FBN2*, *HOXC12*, *CLIP-2*, *LMX1A*, *PDE10A*, *SLC6A2*, *CDH2*, *TLL1*, *NPTX1*, *NTSR1* and *THBD*, were methylated in at least one of the seven pancreatic cancer cell lines but not in either of the ductal epithelial cell lines (Figure 2). Most of these genes were identified as aberrantly methylated for the first time in this study, except for three genes, *HAND1* and *THBD* in stomach cancers (Kaneda *et al.*, 2002), *LMX1* in a colon cancer cell line (Paz *et al.*, 2003), and *ADAM23* in breast cancers (Costa *et al.*, 2004).

Analysis of expression levels of the 27 genes

Expression levels of the 27 genes were analysed by quantitative real-time RT–PCR (primer sequences in Supplementary Table 2) in the two ductal epithelial cell lines and seven pancreatic cancer cell lines (Figure 3). Considering that genes with abundant expression have higher chances of being biologically active, the genes were classified into two groups according to their expression levels in the two ductal epithelial cell lines. Six genes, *RASGRF2*, *PRG2*, *FBN2*, *CDH2*, *NTSR1* and *THBD*, were abundantly expressed in at least one of the two ductal epithelial cell lines, being more than 10^{-3} molecules/*GAPDH* molecules. In all, 11 genes, *ADAM23*, *NEF3*, *OLIG3*, *FGF14*, *NKX2-8*, *HAND1*, *EGR4*, *CLIP2*, *SLC6A2*, *TLL1* and *NPTX1*, were expressed at relatively low levels, with 10^{-4} and 10^{-3} molecules/*GAPDH* molecules. The remaining 10 genes were not expressed at all in either of the two ductal epithelial cell lines.

The correlation between the expression levels and methylation status in the cancer cell lines was examined. All the genes, except *CDH2* and *FGF14*, were either not expressed or very weakly expressed in cancer cell lines with methylations. *CDH2* was expressed in a cancer cell line, BxPC3, in which only methylated DNA molecules were detected by MSP. However, it turned out that, in BxPC3, unmethylated and methylated CpG sites coexisted in the regions for which MSP primers were designed, and that at least partially unmethylated DNA molecules were present (data not shown). *FGF14* showed 'expression' that looked discordant with the methylation status in cell lines. However, the expression levels of *FGF14* in the brain and testes were 100-times as high as those in the two immortalized ductal epithelial cell lines. This strongly suggested that the apparent *FGF14* expression in the pancreatic cancer cell lines and two immortalized ductal epithelial cell lines did not reflect functional levels but was simple leaky expression.

Demethylation and re-expression by 5-aza-dC

To examine the role of methylation of the 5′ CGIs in the loss of gene expression, cancer cells were treated with 5-aza-dC. For all of the six genes with abundant expression, demethylation of their 5′ CGIs induced their re-expression in cancer cell lines that had only methylated DNA molecules (Figure 3). In contrast, re-expression was observed only in seven (*ADAM23*, *NEF3*, *NKX2-8*, *HAND1*, *EGR4*, *TLL1* and *NPTX1*) of the 11 genes with low expression. These results showed that methylation of the 5′ CGIs of the six and seven genes, 13 genes in total, caused their silencing. Since the approach in this study was based on DNA methylation, we were able to identify silencing of genes with low expression levels. As exemplified by *p16* (Figure 3, panel R), some of genes with low expression levels are still important for carcinogenesis.

Analysis of aberrant methylation in primary human pancreatic cancers

In total, 24 primary pancreatic cancers were collected from patients undergoing pancreatectomy with informed consents, and DNA was extracted from the frozen samples. All the cancers were diagnosed as invasive ductal adenocarcinomas (detailed clinical information in Supplementary Table 3). For 18 of the 24 cases, macroscopically normal regions were present in the resected specimens, and noncancerous pancreatic tissues were obtained. Methylation of the 27 5′ CGIs was analysed by MSP in the 24 cancer and 18 noncancerous samples. Among the 13 genes that were silenced by methylation of 5′ regions, methylation was observed for 12 genes: *RASGRF2* (17%), *ADAM23* (29%), *NEF3* (63%), *NKX2-8* (13%), *HAND1* (8%), *EGR4* (4%), *PRG2* (63%), *FBN2* (75%), *CDH2* (29%), *TLL1* (13%), *NPTX1* (13%) and *NTSR1* (8%). Among the four genes that were expressed in the two immortalized ductal epithelial cell lines but whose expression was not restored by 5-aza-dC, methylation

Table 1 List of 40 DNA fragments isolated by MS-RDA from 5′ regions and the downstream genes

DNA fragments isolated by MS-RDA				*Chromosome*	*Genes in the downstream*		*Incidence of methylation*	
Length (bp)	*Accession no.*	*From*	*To*		*Symbols*	*Full names or alternative names*	*Cell lines*	*Primary cancers*
MS-RDA with *Hpa*II								
641	AC026427	170785	171426	5q14	RASGRF2**†	Ras protein-specific guanine nucleotide-releasing factor 2	4/7	4/24
320	AC009225	22726	23046	2q33	ADAM23*†	A disintegrin and a metalloprotease domain 23	4/7	7/24
541	AC008011	24486	25027	12p12	PTHrP	Human parathyroid hormone-related protein	0/6	ND
434	AC096766	117247	117681	4q21	NKX6A	NK6 transcription factor homolog A (pancreatic homeobox)	0/6	ND
513	AL050336	55751	56264	6p12	CLIC5	Chloride intracellular channel 5	0/6	ND
MS-RDA with *Sac*II								
193	AF106564	29260	29453	8p21	NEF3*†	Neurofilament 3	7/7	15/24
299	AL023580	57007	57306	6q23	OLIG3*	Oligodendrocyte transcription factor 3	7/7	¶11/24
103	AL512629	48196	48299	13q34	FGF14 *	Fibroblast growth factor 14 (fibroblast growth factor homologue 4)	7/7	4/24
221	AL132857	3059	3280	14q11	NKX2-8*†	NK2 transcription factor related, locus 8	7/7	3/24
402	AC008971	57542	57944	5p15	SALPR	G-protein-coupled somatostatin and angiotensin-like peptide receptor	6/7	11/24
322	AC067859	139116	139438	18q21	RAX	Retina and anterior neural fold homeobox gene	6/7	¶13/24
633	AL356963	32461	33094	6q25	RGS17	Regulator of G-protein signalling 17	5/7	9/24
574	AC005738	74725	75299	5q31	NGN1	Neurogenin 1	5/7	4/24
367	AC026688	24653	25020	5q33	HAND1*†	Heart and neural crest derives expressed 1	4/7	2/24
513	AC087312	101149	101662	12p11	SOX5	Sex determining region Y - box 5	3/7	3/24
222	AC113194	73722	73944	8q11	RGS20	Regulator of G protein signaling 20	3/7	5/24
517	AC010913	203551	204068	2p12	EGR4*†	Early growth response 4	2/7	1/24
681	AC106781	140502	141183	5q31	ADAMTS19	A disintegrin and a metalloprotease domain, with thrombospondin motif, 19	1/7	2/24
278	AC025483	84337	84615	15q25	SH3GL3	Src homology 3 domain growth factor receptor-bound protein 2 like 3	ND	ND
242	AL109653	144309	144551	Xq27	KIAA1854		ND	ND
MS-RDA with *Nar*I								
280	AC009471	114500	114780	2p25	PRG2**†	p53-responsive gene 2 (PXN, MG50, PRG2, D2S448E, KIAA0230)	7/7	15/24
194	AC113387	119915	120109	5q23	FBN2**†	Fibrillin 2	7/7	18/24
380	AF490843	33251	33631	12q13	HOXC12	Homeo box C12	6/7	0/24
1000	AC011448	99517	100517	19p13	CLIP-2*	Cartilage intermediate layer protein-like protein 2	5/7	0/24
1361	AL160058	14299	15660	1q23	LMX1A	LIM homeobox transcription factor 1 alpha	4/7	3/24
189	AL121789	66583	66772	6q26	PDE10A	Phosphodiesterase 10A	4/7	2/24
724	AC026802	79331	80055	16q13	SLC6A2*	Solute carrier family 6 neurotransmitter transporter noradrenalin member 2	3/7	9/24
594	AC006249	154364	154958	18q11	CDH2**†	Cadherin 2, N-cadherin	3/7	7/24
968	AC097502	124187	125155	4q33	TLL1*†	Tolloid-like 1	3/7	3/24
138	AC120024	64774	64912	17q25	NPTX1*†	Neuronal pentraxin I	3/7	3/24
343	AL357033	72549	72892	20q13	NTSR1**†	Neurotensin receptor 1	2/7	2/24
822	AL495471	3397	4219	20p11	THBD**†	Thrombomodulin	1/7	0/24
523	AC021220	43188	43711	4q11	KDR	Kinase insert domain receptor (VEGFR)	0/7	ND
331	AC015936	141349	141680	17q21	CRF	C1q-related factor	0/7	ND
353	AC092437	81034	81387	4p16	MSX1	Muscle segment homeo box 1 (HOX7(HOMEO BOX 7))	0/7	ND
375	AL159164	59633	60008	6q15	BACH2	BTB (broad complex-tramtrack-bric-a-brac) and CNC (Cap'n'collar) Homology 2	0/7	ND
655	AL078594	65499	66154	6p22	CHF1	Cardiovascular basic-loop–helix factor 1	0/7	ND
543	AC012065	183388	183931	2p24	LOC151449	Similar to growth/differentiation factor 7	ND	ND
829	AC008735	35343	36172	19q13	LOC51157	LDL-induced EC protein	ND	ND
531	AC018735	11753	12284	2q32	LOC151112		ND	ND

Of the 40 CGIs flanked by the DNA fragments, 35 CGIs were analysed for their methylation status, and 27 CGIs were found to be methylated in one or more cell lines. Expression analysis of the 27 downstream genes showed that 17 of them were expressed **abundantly or *slightly in pancreatic ductal epithelial cell lines. Treatment with 5-aza-dC indicated that 13 of them (shown by †) were silenced in cancer cell lines. ¶Methylation in noncancerous tissue was observed. ND: not done

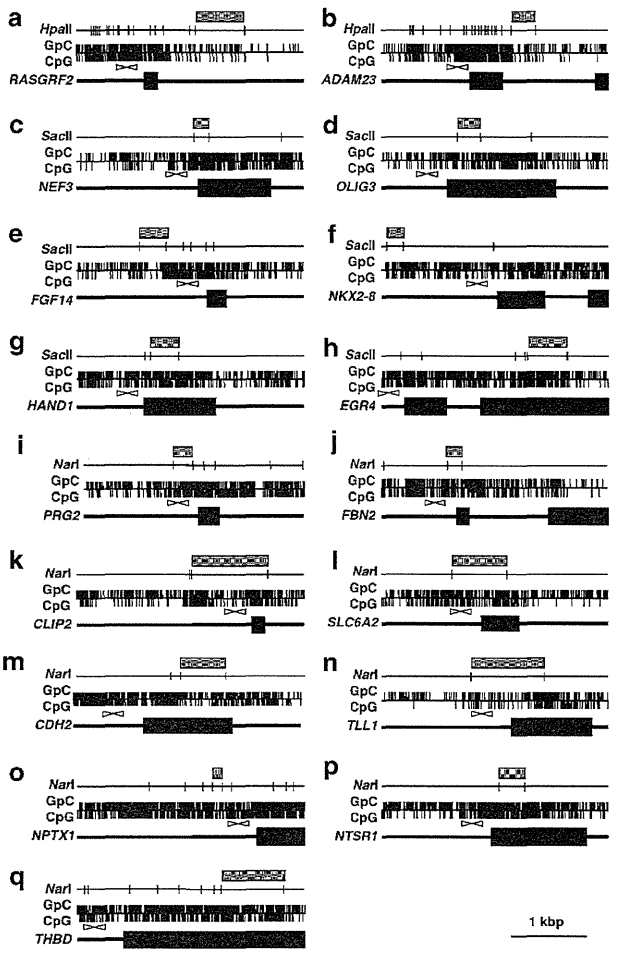

Figure 1 Genomic structures around the 17 5′ CGIs whose downstream genes were expressed in the two ductal epithelial cell lines. GpC, CpG and recognition sites for the restriction enzyme used for MS-RDA are shown. CGIs can be identified by comparing the densities of GpC and CpG sites. Closed and shaded boxes show exons and the DNA fragments isolated by MS-RDA, respectively. Arrow heads show the positions of MSP primers

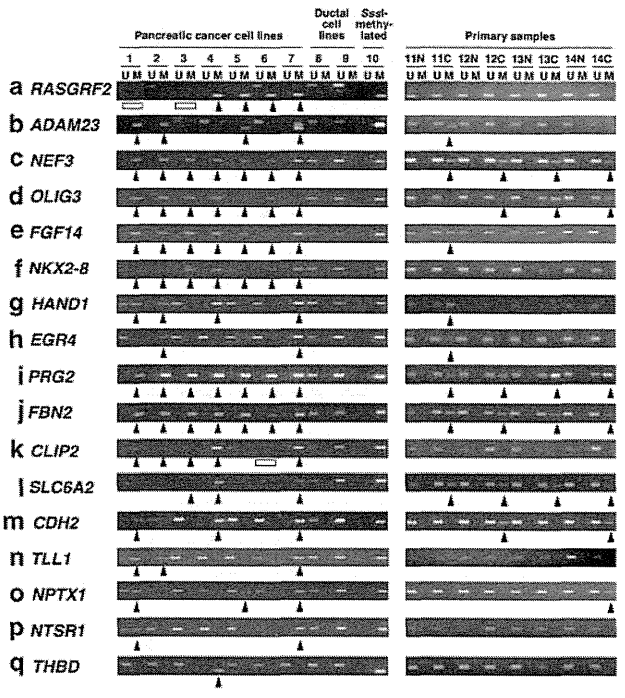

Figure 2 Methylation statuses of the 17 5′ CGIs whose downstream genes were expressed in the two ductal epithelial cell lines. Methylation statuses were first analysed in seven pancreatic cancer cell lines (1: BxPC3, 2: HPAF-II, 3: Capan-2, 4: MIA PaCa-2, 5: Hs766T, 6: PANC-1, 7: HPAC) and two immortalized pancreatic ductal epithelial cell lines (8: HPDE6-E6E7c7, 9: HPDE-4/E6E7). 10: *Sss*I-methylated DNA of HPDE-4/E6E7. Then, CGIs methylated in at least one cell line were analysed in 24 primary pancreatic cancers and 18 noncancerous tissues. Results on four representative paired samples are shown here (1–14: N, noncancerous tissue; C, cancer). Genomic DNA was treated with bisulfite as reported (Kaneda *et al*., 2002), and was amplified using primer sets specific to methylated and unmethylated genomic DNA (M and U sets, respectively). Closed arrows show bands obtained with the M primer set. Rectangles show regions where no PCR products were obtained using the U or M primer sets, indicating homozygous deletion

in at least one primary cancer was observed for three genes; *CLIP2* was the exception. Of the 10 genes that were not expressed in the two immortalized ductal epithelial cell lines, methylation was observed for nine.

Of the 27 aberrantly methylated 5′ CGIs, only those of *OLIG3* and *RAX* showed methylation in the 18 noncancerous samples. Methylation is reported to be often detected even in noncancerous samples (Ueki *et al*., 2001). The low incidence in this study was in contrast, and was considered to be due to the region analysed and to the analytical method employed. To search for a region in a CGI that is consistently unmethylated in the two immortalized ductal epithelial cell lines, we tried multiple regions in the CGI. For MSP, we first determined the number of PCR cycles that would produce a minimal band with 100%-methylated DNA (DNA treated with *Sss*I-methylase), and four more cycles were added for the test samples.

Included among the 12 genes that were silenced in pancreatic cancer cell lines and methylated in primary pancreatic cancers were genes that can be potentially involved in pancreatic cancer development and progression. *RASGRF2* was deleted in two cell lines (BxPC3 and Capan-2, Figure 2). *RASGRF2* has been reported to be involved in H-Ras signalling (Arozarena *et al*., 2004), and its expression to be decreased in rat mammary carcinomas (Qiu *et al*., 2003). Frequent epigenetic silencing of *ADAM23* was recently reported in breast cancers (Costa *et al*., 2004). *PRG2* is located on chromosome 2pter–p25, and loss of heterozygosity at this locus is reported in pancreatic cancers (Griffin *et al*., 1994). Its shorter variant is highly expressed in cells undergoing apoptosis due to p53 overexpression (Horikoshi *et al*., 1999), and its longer variant, *MG50*, is strongly immunogenic to human cytolytic T lymphocytes (Mitchell *et al*., 2000). Silencing of the *PRG2*/*MG50* gene could confer a growth advantage to a cell by allowing it to escape from immune surveillance and/or p53-dependent apoptosis. N-cadherin, coded by *CDH2*,

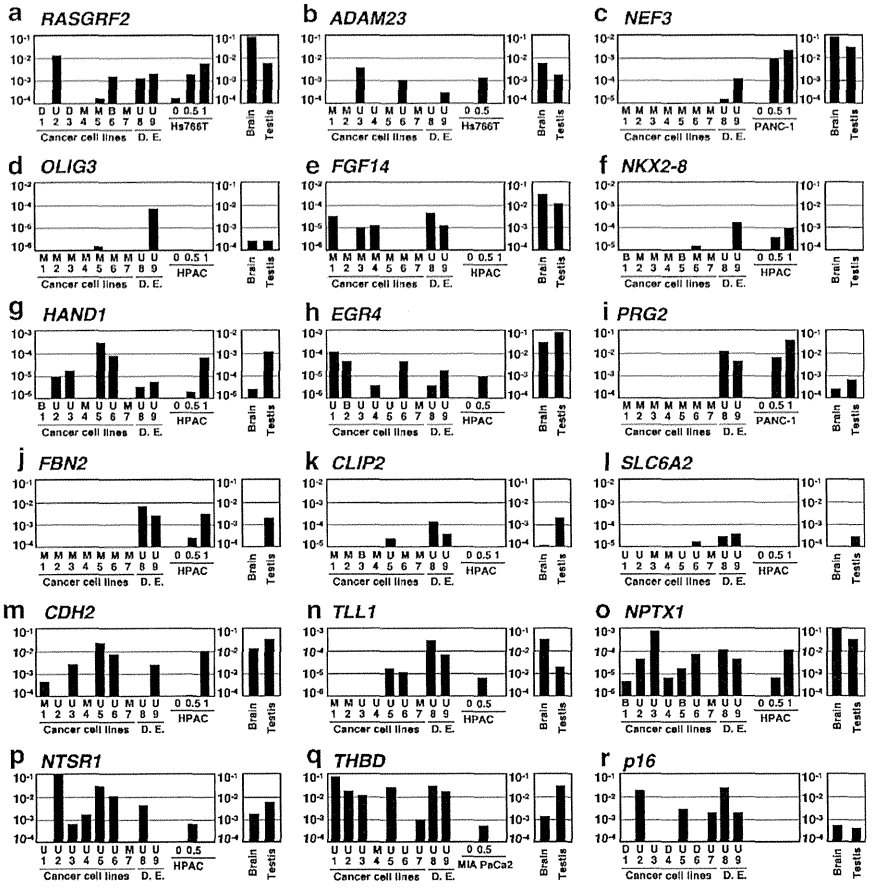

Figure 3 Expression levels of the 17 genes and the *p16* gene. Expression levels were analysed in the seven cancer cell lines, two pancreatic ductal epithelial cell lines, and cancer cell lines after 5-aza-dC treatment. Those in the brain and testes were also analysed. 1: BxPC3, 2: HPAF-II, 3: Capan-2, 4: MIA PaCa-2, 5: Hs766T, 6: PANC-1, 7: HPAC, 8: HPDE6-E6E7c7, 9: HPDE-4/E6E7. 0, 0.5 and 1 stand for concentrations of 5-aza-dC treatment. cDNA was synthesized from 3 μg of total RNA using a Superscript II kit (Invitrogen) after DNase treatment. The numbers of cDNA molecules were quantified using SYBR Green PCR Core Reagents (PE Applied Biosystems, Foster City, CA, USA) and an iCycler Thermal Cycler (Bio-Rad Laboratories, Hercules, CA, USA), and were normalized to that of *GAPDH* cDNA molecules. Six genes, *RASGRF2*, *PRG2*, *FBN2*, *CDH2*, *NTSR1* and *THBD* genes (panels A, I, J, M, P and Q, respectively), were found to be expressed at levels higher than 1/1000 of *GAPDH* in one or both of the two ductal epithelial cell lines, and the other 11 genes were expressed at low levels in the two ductal epithelial cell lines. The expressions of the six abundantly expressed genes and seven of the 11 weakly expressed genes were restored by 5-aza-dC treatment, demonstrating their silencing by methylation. Results of MSP in Figure 2 are noted by U (bands obtained only by U primer set), M (bands obtained only by M primer set), B (bands obtained by both U and M primer sets), and D (no bands obtained by either U or M primer sets). Closed arrows show bands obtained with the M primer set

was recently reported to function in the downstream of the *RASSF1A* tumor-suppressor gene (Agathanggelou *et al*., 2003), and its silencing could confer a growth advantage.

In contrast, genes that are unlikely to be involved in pancreatic cancer development and progression were also present among the 13 silenced genes. *NEF3* and *NPTX1* are known to be functionally expressed in the brain (Omeis *et al*., 1996; Julien and Mushynski, 1998), and *EGR4* is functionally expressed in the testes (Tourtellotte *et al*., 1999). *HAND1* is essential for placental development (Riley *et al*., 1998), and *TLL1* plays multiple roles in heart development (Clark *et al*., 1999). The expression levels of *NEF3*, *HAND1*, *EGR4*, *TLL1* and *NPTX1* were lower than 1/100 of those in the brain or testes. In addition, 10 genes whose 5′ CGIs were methylated in pancreatic cancer cell lines were not expressed at all in the two immortalized ductal epithelial cell lines. These suggested that genes with low or no expression tended to be silenced by promoter methylation.

In summary, we identified 27 aberrantly methylated 5′ CpG islands and 13 genes silenced by methylation of the 5′ CGIs, and most of them were novel.

Abbreviations

CGI, CpG island; MS-RDA, methylation-sensitive representational difference analysis; MSP, methylation-specific PCR; RT–PCR, reverse-transcription–PCR; 5-aza-dC, 5-aza-2′-deoxycytidine.

Acknowledgements

The authors are grateful to Drs M Sakamoto and B Nakata for providing tumor samples; and to Dr N McDonell for critical reading of the manuscript. This work was supported by

Grants-in-Aid for the Second-term Comprehensive 10-Year Strategy for Cancer Control; by the Special Coordination Funds for Promoting Science and Technology from the Ministry of Education, Culture, Sports, Science and Technology (MEXT), Japan; and by a Grant from the Foundation for Promotion of Cancer Research. AH and JF are recipients of Research Resident Fellowships from the Foundation for Promotion of Cancer Research.

References

Agathanggelou A, Bieche I, Ahmed-Choudhury J, Nicke B, Dammann R, Baksh S, Gao B, Minna JD, Downward J, Maher ER and Latif F. (2003). *Cancer Res.*, **63,** 5344–5351.

Almoguera C, Shibata D, Forrester K, Martin J, Arnheim N and Perucho M. (1988). *Cell*, **53,** 549–554.

Arozarena I, Matallanas D, Berciano MT, Sanz-Moreno V, Calvo F, Munoz MT, Egea G, Lafarga M and Crespo P. (2004). *Mol. Cell. Biol.*, **24,** 1516–1530.

Asada K, Miyamoto K, Fukutomi T, Tsuda H, Yagi Y, Wakazono K, Oishi S, Fukui H, Sugimura T and Ushijima T. (2003). *Oncology*, **64,** 380–388.

Bardeesy N and DePinho RA. (2002). *Nat. Rev. Cancer*, **2,** 897–909.

Caldas C, Hahn SA, da Costa LT, Redston MS, Schutte M, Seymour AB, Weinstein CL, Hruban RH, Yeo CJ and Kern SE. (1994). *Nat. Genet.*, **8,** 27–32.

Clark TG, Conway SJ, Scott IC, Labosky PA, Winnier G, Bundy J, Hogan BL and Greenspan DS. (1999). *Development*, **126,** 2631–2642.

Costa FF, Verbisck NV, Salim AC, Ierardi DF, Pires LC, Sasahara RM, Sogayar MC, Zanata SM, Mackay A, O'Hare M, Soares F, Simpson AJ and Camargo AA. (2004). *Oncogene*, **23,** 1481–1488.

Furukawa T, Duguid WP, Rosenberg L, Viallet J, Galloway DA and Tsao MS. (1996). *Am. J. Pathol.*, **148,** 1763–1770.

Griffin CA, Hruban RH, Long PP, Morsberger LA, Douna-Issa F and Yeo CJ. (1994). *Genes Chromosomes Cancer*, **9,** 93–100.

Hahn SA, Schutte M, Hoque AT, Moskaluk CA, Da Costa LT, Rozenblum E, Weinstein CL, Fischer A, Yeo CJ, Hruban RH and Kern SE. (1996). *Science*, **271,** 350–353.

Herman JG, Merlo A, Mao L, Lapidus RG, Issa JP, Davidson NE, Sidransky D and Baylin SB. (1995). *Cancer Res.*, **55,** 4525–4530.

Horikoshi N, Cong J, Kley N and Shenk T. (1999). *Biochem. Biophys. Res. Commun.*, **261,** 864–869.

Jemal A, Murray T, Samuels A, Ghafoor A, Ward E and Thun MJ. (2003). *CA Cancer J. Clin.*, **53,** 5–26.

Julien JP and Mushynski WE. (1998). *Prog. Nucleic Acid Res. Mol. Biol.*, **61,** 1–23.

Kaneda A, Kaminishi M, Yanagihara K, Sugimura T and Ushijima T. (2002). *Cancer Res.*, **62,** 6645–6650.

Kaneda A, Takai D, Kaminishi M, Okochi E and Ushijima T. (2003). *Ann. NY Acad. Sci.*, **983,** 131–141.

Lisitsyn N and Wigler M. (1993). *Science*, **259,** 946–951.

Liu N, Furukawa T, Kobari M and Tsao MS. (1998). *Am. J. Pathol.*, **153,** 263–269.

Merlo A, Herman JG, Mao L, Lee DJ, Gabrielson E, Burger PC, Baylin SB and Sidransky D. (1995). *Nat. Med.*, **1,** 686–692.

Mitchell MS, Kan-Mitchell J, Minev B, Edman C and Deans RJ. (2000). *Cancer Res.*, **60,** 6448–6456.

Miyamoto K, Asada K, Fukutomi T, Okochi E, Yagi Y, Hasegawa T, Asahara T, Sugimura T and Ushijima T. (2003). *Oncogene*, **22,** 274–280.

Omeis IA, Hsu YC and Perin MS. (1996). *Genomics*, **36,** 543–545.

Paz MF, Wei S, Cigudosa JC, Rodriguez-Perales S, Peinado MA, Huang TH and Esteller M. (2003). *Hum. Mol. Genet.*, **12,** 2209–2219.

Qiu C, Yu M, Shan L and Snyderwine EG. (2003). *Oncogene*, **22,** 1253–1260.

Riley P, Anson-Cartwright L and Cross JC. (1998). *Nat. Genet.*, **18,** 271–275.

Rozenblum E, Schutte M, Goggins M, Hahn SA, Panzer S, Zahurak M, Goodman SN, Sohn TA, Hruban RH, Yeo CJ and Kern SE. (1997). *Cancer Res.*, **57,** 1731–1734.

Sato N, Fukushima N, Maitra A, Matsubayashi H, Yeo CJ, Cameron JL, Hruban RH and Goggins M. (2003). *Cancer Res.*, **63,** 3735–3742.

Takai D and Jones PA. (2002). *Proc. Natl. Acad. Sci. USA*, **99,** 3740–3745.

Takai D, Yagi Y, Wakazono K, Ohishi N, Morita Y, Sugimura T and Ushijima T. (2001). *Oncogene*, **20,** 7505–7513.

Tourtellotte WG, Nagarajan R, Auyeung A, Mueller C and Milbrandt J. (1999). *Development*, **126,** 5061–5071.

Toyota M, Ho C, Ahuja N, Jair KW, Li Q, Ohe-Toyota M, Baylin SB and Issa JP. (1999). *Cancer Res.*, **59,** 2307–2312.

Ueki T, Toyota M, Skinner H, Walter KM, Yeo CJ, Issa JP, Hruban RH and Goggins M. (2001). *Cancer Res.*, **61,** 8540–8546.

Ueki T, Toyota M, Sohn T, Yeo CJ, Issa JP, Hruban RH and Goggins M. (2000). *Cancer Res.*, **60,** 1835–1839.

Ushijima T, Morimura K, Hosoya Y, Okonogi H, Tatematsu M, Sugimura T and Nagao M. (1997). *Proc. Natl. Acad. Sci. USA*, **94,** 2284–2289.

Wilentz RE, Iacobuzio-Donahue CA, Argani P, McCarthy DM, Parsons JL, Yeo CJ, Kern SE and Hruban RH. (2000). *Cancer Res.*, **60,** 2002–2006.

Supplementary information is available at ONC reports online (http://www.nature.com/onc)

OXFORD

Carcinogenesis, 2015, Vol. 36, No. 2, 192–201

doi:10.1093/carcin/bgu238
Advance Access publication December 4, 2014
Original Manuscript

ORIGINAL MANUSCRIPT

Identification of coexistence of DNA methylation and H3K27me3 specifically in cancer cells as a promising target for epigenetic therapy

Hideyuki Takeshima, Mika Wakabayashi, Naoko Hattori, Satoshi Yamashita and Toshikazu Ushijima*

Division of Epigenomics, National Cancer Center Research Institute, 5-1-1 Tsukiji, Chuo-ku, Tokyo 104-0045, Japan

*To whom correspondence should be addressed. Tel: +81 3 3547 5240; Fax: +81 3 5565 1753; Email: tushijim@ncc.go.jp

Abstract

Alterations of epigenetic modifications are promising targets for cancer therapy, and several epigenetic drugs are now being clinically utilized. At the same time, individual epigenetic modifications have physiological functions in normal cells, and cancer cell specificity is considered difficult to achieve using a drug against a single epigenetic modification. To overcome this limitation, a combination of epigenetic modifications specifically or preferentially present in cancer cells is a candidate target. In this study, we aimed to demonstrate (i) the presence of a cancer cell-specific combination of epigenetic modifications by focusing on DNA methylation and trimethylation of histone H3 lysine 27 (H3K27me3) and (ii) the therapeutic efficacy of a combination of DNA demethylation and EZH2 inhibition. Analyses of DNA methylation and H3K27me3 in human colon, breast and prostate cancer cell lines revealed that 24.7±4.1% of DNA methylated genes had both DNA methylation and H3K27me3 (dual modification) in cancer cells, while it was 11.8±7.1% in normal cells. Combined treatment with a DNA demethylating agent, 5-aza-2′-deoxycytidine (5-aza-dC) and an EZH2 inhibitor, GSK126, induced marked re-expression of genes with the dual modification, including known tumor-suppressor genes such as *IGFBP7* and *SFRP1*, and showed an additive inhibitory effect on growth of cancer cells *in vitro*. Finally, an *in vivo* combined treatment with 5-aza-dC and GSK126 inhibited growth of xenograft tumors more efficiently than a single treatment with 5-aza-dC. These results showed that the dual modification exists specifically in cancer cells and is a promising target for cancer cell-specific epigenetic therapy.

Introduction

Epigenetic alterations, including aberrant DNA methylation and alterations in histone modifications, are frequently present in human cancers (1,2), and are promising targets for cancer therapy (3,4). Currently, DNA demethylating agents, 5-azacytidine (azacitidine) and 5-aza-2′-deoxycytidine (decitabine; 5-aza-dC), are clinically being utilized for patients with myelodysplastic syndromes (5–7), and histone deacetylase (HDAC) inhibitors, vorinostat and romidepsin, are utilized for patients with cutaneous T-cell lymphoma (8). Not only in hematological malignancies but also in solid tumors, multiple trials of these epigenetic drugs have been conducted, and the efficacy has been shown, at least in non-small cell lung cancers (9). In addition, inhibitors of various histone methyltransferases, such as DOT1L (EPZ004777), EZH2 (EI1, EPZ-6438 and GSK126) and G9a (BIX-01294), have been developed, and their efficacies have been demonstrated in preclinical studies (10–14).

Among the various epigenetic modifications, DNA methylation and trimethylation of histone H3 lysine 27 (H3K27me3) have critical roles in carcinogenesis. DNA methylation of promoter CpG islands (CGIs) is involved in the repression of tumor-suppressor genes, such as *BRCA1*, *CDKN2A* (p16) and *RASSF1A* genes (15–17). H3K27me3 is involved in the repression of tumor-suppressor genes, such as *CDH1* (E-cadherin) and *DKK1* (18,19), independently of DNA methylation (20). At the same time,

Received: March 8, 2014; **Revised:** November 6, 2014; **Accepted:** November 26, 2014

Abbreviations

5-Aza-dC	5-aza-2′-deoxycytidine
CGI	CpG island
HDAC	histone deacetylase
H3K27me3	trimethylation of histone H3 lysine 27
PBS	phosphate-buffered saline
TSS	transcription start site

individual epigenetic modifications, including DNA methylation and H3K27me3, have physiological functions in normal cells (21,22), such as repression of transposable elements and genes required for embryonic development and cellular differentiation (23,24). Therefore, cancer cell specificity is considered difficult to achieve using a drug against a single epigenetic modification.

To overcome this limitation, a combination of epigenetic modifications specifically or preferentially present in cancer cells is a potential target. As a candidate for such a combination, we here focused on DNA methylation and H3K27me3 because of their functional crosstalk during carcinogenesis. Namely, H3K27me3 in normal cells functions as a premark of aberrant DNA methylation induction in cancer cells and also in normal-appearing tissues exposed to chronic inflammation (25–30). Switching of repression by H3K27me3 to that by DNA methylation is frequently observed for various genes during carcinogenesis (31). Since DNA methylation and H3K27me3 exist in a mutually exclusive manner in embryonic stem cells and normal cells (32,33), a failure in switching may generate a cancer cell-specific combination of epigenetic modifications, DNA methylation and H3K27me3. Indeed, it was recently reported that a combination of DNA methylation and H3K27me3 is specifically present in cancer cells (34).

In this study, we will first confirm the cancer cell specificity of the combination of DNA methylation and H3K27me3. Then, to reveal the potential of this combination as a target for cancer cell-specific epigenetic therapy, we will show whether or not a combination of DNA demethylation and EZH2 inhibition is effective for (i) re-expression of genes with both DNA methylation and H3K27me3 and (ii) inhibition of cancer cell growth *in vitro* and *in vivo*.

Materials and methods

Cell lines and drug treatment

Human prostate cancer cell lines (Du145 and PC3), breast cancer cell lines (MCF7 and MDA-MB-231), colon cancer cell lines (HCT116 and RKO), a normal prostatic epithelial cell line (RWPE1) and normal human colon epithelial cells (FHC) were purchased from the American Type Culture Collection (Rockville, MD). Normal human mammary epithelial cells were purchased from Cambrex (East Rutherford, NJ).

PC3 and MCF7 were seeded on day 0, and were treated (i) with 5-aza-dC (Sigma–Aldrich, St. Louis, MO) and/or GSK126 (Active Biochem, Maplewood, NJ) and (ii) with 5-aza-dC and/or entinostat (ChemScene, Monmouth Junction, NJ) for 4 days. Cell numbers were counted on day 5, and the cells were harvested. For 5-aza-dC and GSK126, drug concentrations used in the combined treatment were determined based on the inhibitory effect on DNA methylation (5-aza-dC) or H3K27me3 (GSK126) (Supplementary Figures 1A and 2A is available at *Carcinogenesis* Online). The selected doses of 5-aza-dC showed inhibitory effects on cell growth similar to the neighboring doses (Supplementary Figure 1B is available at *Carcinogenesis* Online). The selected dose of GSK126 showed a mild inhibitory effect on cell growth (Supplementary Figure 2B is available at *Carcinogenesis* Online). For entinostat, drug concentration used in the combined treatment was determined based on the inhibitory effect on cell growth. The selected dose of entinostat showed a mild inhibitory effect on cell growth (Supplementary Figure 3 is available at *Carcinogenesis* Online).

Genomic DNA was extracted by the standard phenol/chloroform method, and was quantified using a Quant-iT PicoGreen dsDNA Assay Kit (Life Technologies, Carlsbad, CA). Total RNA was extracted from cancer cell lines and their normal counterpart cells using ISOGEN (Nippon Gene, Tokyo, Japan).

Analysis of DNA methylation

Genome-wide analysis of DNA methylation was performed using an Infinium HumanMethylation450 BeadChip array (Illumina, San Diego, CA) as described previously (35). The DNA methylation level of an individual probe (CpG site) was obtained as the β value that ranged from 0 (unmethylated) to 1 (fully methylated). A total of 482 421 CpG sites were assembled into 296 494 genomic blocks, collections of CpG sites which were classified by their locations from transcription start sites (TSSs) [TSS1500 (regions between 200 bp upstream and 1500 bp upstream from TSS), TSS200 (a 200-bp upstream region from TSS), 5′-UTR, the 1st exon, the gene body, 3′-UTR and an intergenic region] and their relative location against a CGI (N Shelf, N Shore, CGI, S Shore, S Shelf and non-CGI) (35). Among the 296 494 genomic blocks, 61 422 were located in CGIs and 7384 of them were located in TSS200 (TSS200 CGIs). Individual TSS200 CGIs contained 1–14 (average 3.5±1.8) CpG sites, whose DNA methylation levels can be detected by a BeadChip array. The DNA methylation level of an individual TSS200 CGI (individual gene) was evaluated using the mean β value of all the CpG sites within an individual TSS200 CGI. Genes with β values of 0.9 or more and those of 0.2 or less were defined as methylated and unmethylated genes, respectively. Genes with β values of 0.2–0.9 were considered as partially methylated genes.

Gene-specific analysis of DNA methylation was performed by quantitative methylation-specific PCR and bisulfite sequencing. Quantitative methylation-specific PCR was performed using primers specific to methylated or unmethylated DNA (Supplementary Table 1 is available at *Carcinogenesis* Online) and DNA methylation levels were calculated as [number of methylated molecules/number of the total DNA molecules (methylated molecules + unmethylated molecules) × 100]. Bisulfite sequencing was performed using universal primers for methylated and unmethylated DNA sequences (Supplementary Table 2 is available at *Carcinogenesis* Online). The PCR product was cloned into pGEM-T Easy vector (Promega, Madison, WI), and sequenced using a DYEnamic ET Terminator Cycle Sequencing kit (GE Healthcare, Buckinghamshire, UK) and an ABI PRISM 310 sequencer (PE Biosystems, Foster City, CA).

Analysis of H3K27me3

Chromatin immunoprecipitation for H3K27me3 was performed as described previously (29). Briefly, 30 μg of chromatin extracted from cross-linked cells was immunoprecipitated using 2 μg of antibody against H3K27me3 (07-449, Millipore, Billerica, MA). Immunoprecipitated chromatin was treated with RNaseA and proteinase K, and DNA was recovered by phenol/chloroform extraction and isopropanol precipitation. The precipitated DNA was dissolved in 30 μl of 1× TE (10 mM Tris–HCl, pH 8.0, 1 mM ethylenediaminetetraacetic acid).

Genome-wide analysis of H3K27me3 was performed using a human CGI oligonucleotide microarray (Agilent technologies, Santa Clara, CA) as described previously (29). H3K27me3 levels (Bound signal/Input signal) of individual genes were evaluated using genomic blocks used for DNA methylation analysis (by a BeadChip array). CGI microarray probes located within 100 bp from any BeadChip array probes in a genomic block were assigned to the genomic block (Supplementary Figure 4 is available at *Carcinogenesis* Online). The position of a CGI microarray probe was defined by the center position of a probe. The H3K27me3 level of an individual genomic block was evaluated using the mean H3K27me3 level of all the probes assigned to a genomic block. Genomic blocks whose H3K27me3 levels were 1.5 or more were defined as those with H3K27me3.

Analysis of H3K27me3 levels of individual genes was performed by ChIP-quantitative PCR as described previously (29) using primers listed in Supplementary Table 3 is available at *Carcinogenesis* Online. Analysis of DNA methylation of chromatin immunoprecipitated DNA was performed using 19 of 30 μl of immunoprecipitated DNA.

Analysis of gene expression

Genome-wide analysis of gene expression was performed using a SurePrint G3 Human GE Microarray 8×60K v2 (Agilent Technologies). From 200 ng

of total RNA, Cy3-labeled cRNA was synthesized using a Low Input Quick Amp Labeling Kit (Agilent Technologies) and 600 ng of labeled cRNA was fragmented and hybridized to a microarray. The microarray was scanned with an Agilent G2565BA microarray scanner (Agilent Technologies). The scanned data were processed using Feature Extraction Ver.10.7 software (Agilent Technologies), and analyzed using GeneSpring Ver.12.5 software (Agilent Technologies). The signal intensity of each probe was normalized so that the 75th percentile of signal intensity of all the probes would be 1.0. Mean signal intensity of all the probes within a gene was used as its expression level, and genes with signal intensities of 0.5 or more were considered to be expressed. Analysis of gene expression levels of individual genes was performed by quantitative RT-PCR as described previously (29) using primers listed in Supplementary Table 4 is available at *Carcinogenesis* Online.

Immunofluorescence

Cells were fixed with 4% formaldehyde and permeabilized by 1% Triton X-100 in 1× phosphate-buffered saline (PBS) (–). The cells were incubated in blocking buffer [1% bovine serum albumin in 1× PBS (–)], and then incubated with rabbit polyclonal antibody against H3K27me3 (1:1000; 07-449; Millipore) and mouse monoclonal antibody against histone H3 (1:1000; 300–34783; Wako, Tokyo, Japan). After washing with 1× PBS (–), cells were incubated with Alexa Fluor 594-conjugated goat anti-rabbit IgG (1:1000, Life Technologies) and Alexa Fluor 488-conjugated goat anti-mouse IgG (1:1000, Life Technologies). After washing with 1× PBS (–), coverslips were mounted using ProLong Gold antifade reagent with DAPI (Life Technologies). Fluorescence of stained cells was detected using a BZ-9000 microscope system (Keyence, Osaka, Japan).

Western blotting

Proteins in total cell lysate were separated by sodium dodecyl sulfate–polyacrylamide gel electrophoresis, and were transferred to a polyvinylidene difluoride membrane (Millipore). H3K27me3, histone H3 and EZH2 were detected using rabbit polyclonal antibody against H3K27me3 (1:1000; 07-449; Millipore), rabbit polyclonal antibody against histone H3 (1:5000; ab1791; Abcam, Cambridge, UK) and mouse monoclonal antibody against EZH2 (1:1000; 3147S; Cell Signaling Technology, Danvers, MA), respectively. Protein bands were quantified by using ImageJ 1.47v software.

Xenograft tumor formation assay in nude mice

PC3 cells (1.5×10^6 cells) were inoculated subcutaneously into 6-week-old male nude mice (BALB/cAJc1-nu/nu; CLEA Japan, Tokyo, Japan). 5-Aza-dC (0.2 mg/kg) and/or GSK126 (10 or 15 mg/kg) were intraperitoneally administrated three times per week. The length and width of tumors were measured using calipers and the tumor volume was calculated as [(length × width^2) × 0.5]. After 8 weeks, tumors were collected for the measurement of tumor weights, and total blood was collected for the analysis of the number of leukocytes, erythrocytes and platelets. All the animal experiments were approved by the Committee for Ethics in Animal Experimentation at the National Cancer Center.

Statistical analysis

The differences in H3K27me3 levels were evaluated by the Mann–Whitney *U*-test. The differences in cell growth were evaluated by the Student's *t*-test.

Gene ontology analysis

Gene ontology analysis was performed by DAVID bioinformatics resources (36,37) as described previously (29). The enrichment of genes in a biological process was analyzed by comparing a fraction of genes with an ontology among genes with gain (or loss) of H3K27me3 in cancer cells with that among all the genes with TSS200 CGIs.

Results

Increase of genes with both DNA methylation and H3K27me3 in cancer cells

DNA methylation status was compared between cancer cell lines and their normal counterpart cells in the colon, mammary glands, and prostate for 61 422 genomic blocks with CGIs. Bimodal distribution of DNA methylation levels was observed in both cancer cell lines and normal cells, but the number of methylated blocks was larger in cancer cell lines than in normal cells (Figure 1A). When the analysis was limited to 7384 TSS200 CGIs, the six cancer cell lines had methylation of 238–969 genes while normal cells had that of only 55–75 genes (Supplementary Table 5 is available at *Carcinogenesis* Online).

Then, H3K27me3 status was compared between cancer cell lines and normal cells. The numbers of genomic blocks (Figure 1B) and TSS200 CGIs (Supplementary Table 5 is available at *Carcinogenesis* Online) with H3K27me3 were similar between cancer (743–1165 TSS200 CGIs) and normal cells (576–973 TSS200 CGIs). When the changes of H3K27me3 status were analyzed, 331–645 and 254–554 TSS200 CGIs showed gain and loss, respectively, of H3K27me3 in cancer cells (Supplementary Table 6 is available at *Carcinogenesis* Online). Genes with gain of H3K27me3 tended to have gene functions related to cell communication and cell–cell signaling. In contrast, genes with loss of H3K27me3 tended to have gene functions related to development (Supplementary Table 7 is available at *Carcinogenesis* Online).

Overlap between genes with DNA methylation and those with H3K27me3 was then analyzed. In cancer cell lines, 24.7 ± 4.1% of methylated genes (49–248 genes) had both DNA methylation and H3K27me3 (dual modification). On the other hand, in normal cells, only 11.8 ± 7.1% of DNA methylated genes (4–12 genes) had the dual modification (Figure 1C). Among the genes with the dual modification, known tumor-suppressor genes, such as *IGFBP7* and *SFRP1* (38–40), were present (Supplementary Table 8 is available at *Carcinogenesis* Online). These results showed that the fraction of genes with the dual modification was increased in cancer cells compared with their normal counterpart cells.

The existence of DNA methylation and H3K27me3 on the same DNA molecules

The existence of DNA methylation and H3K27me3 on the same DNA molecules was analyzed in two cancer cell lines, PC3 and MCF7, by bisulfite sequencing of chromatin immunoprecipitated DNA (32,41). First, higher H3K27me3 levels were confirmed in the genes with the dual modification, *CNN3*, *SFRP1* and *SLC6A15*, than in housekeeping genes, *EEF1A1* and *GAPDH* (Figure 2A). Then, the DNA methylation status of the DNA molecules immunoprecipitated by anti-H3K27me3 antibody was analyzed. All the DNA molecules sequenced were densely methylated at promoter CGIs of these genes (Figure 2B). The result showed that DNA methylation and H3K27me3 coexisted on the same DNA molecules.

High H3K27me3 levels in normal cells for genes with the dual modification

DNA methylation and H3K27me3 status in normal counterpart cells were analyzed for genes with the dual modification and genes with only DNA methylation. H3K27me3 was present in normal cells for 54.6 ± 14.4% (20–150 genes) of genes with the dual modification in cancer cell lines and for 28.1 ± 7.3% (34–266 genes) of genes with only DNA methylation (Supplementary Table 9 is available at *Carcinogenesis* Online). When the H3K27me3 level was analyzed, it was significantly higher in genes with the dual modification than in genes with only DNA methylation (Figure 3). Neither DNA methylation nor H3K27me3 was present in normal cells for 29.9 ± 17.4% (4–104 genes) of genes with the dual modification in cancer cell lines and for 37.0 ± 16.8% (20–363 genes) of genes with only DNA methylation (Supplementary

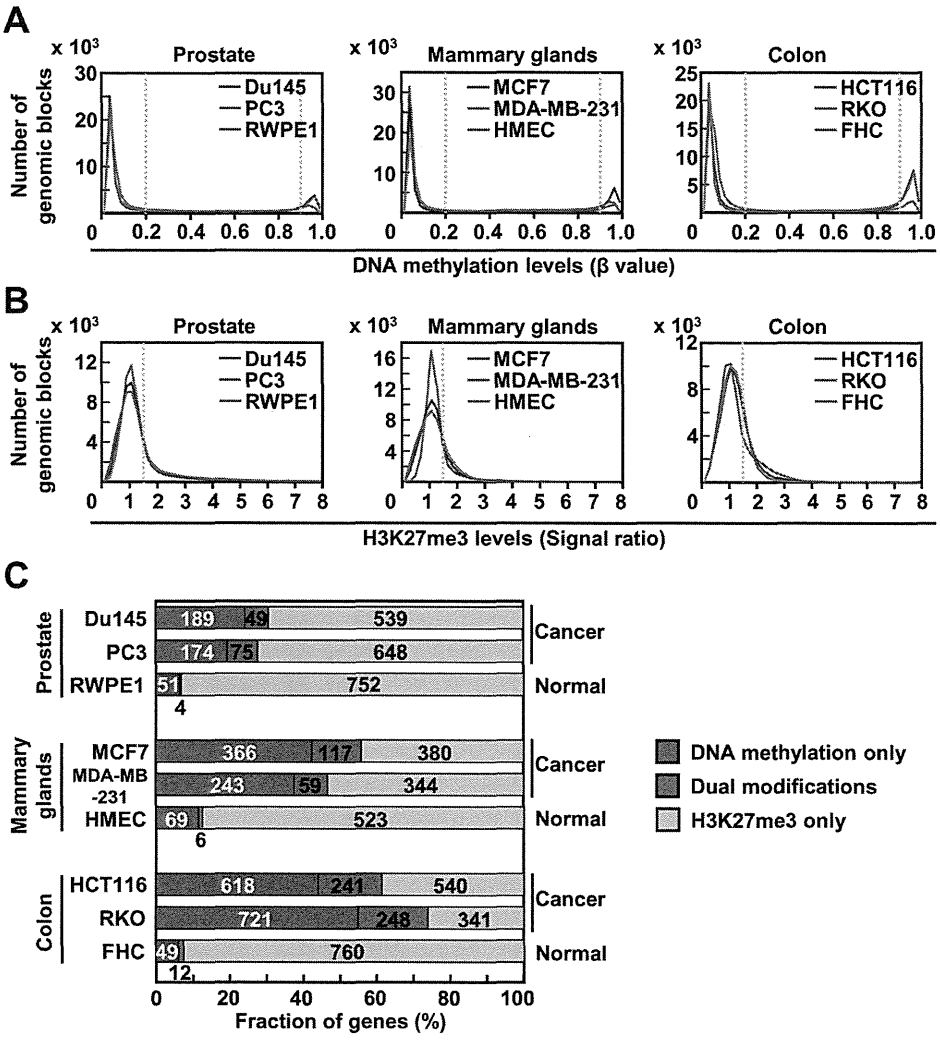

Figure 1. Increase of genes with DNA methylation and H3K27me3 (dual modification) in cancer cells. (**A**) Distribution of DNA methylation levels of 61 422 genomic blocks with CGIs. The number of methylated blocks was larger in cancer cell lines (Du145, PC3, MCF7, MDA-MB-231, HCT116 and RKO) than in their normal counterpart cells (RWPE1, HMEC and FHC). (**B**) Distribution of H3K27me3 levels of 56 523 genomic blocks with CGIs. The distribution of H3K27me3 levels was similar among cancer cell lines in each tissue. (**C**) Overlap of genes with DNA methylation and those with H3K27me3. The fraction of genes with the dual modification was increased in cancer cell lines compared with their normal counterpart cells.

Table 9 is available at *Carcinogenesis* Online). These results showed that genes with the dual modification frequently had high H3K27me3 levels in normal counterpart cells.

The repressive effect of the dual modification on gene expression

To analyze the effect of the dual modification on gene expression, the expression levels of the genes with the dual modification were compared with (i) those of genes with only DNA methylation, (ii) those of genes with only H3K27me3 and (iii) those of genes without DNA methylation or H3K27me3. The genes with the dual modification had the lowest expression levels, along with the genes with only DNA methylation, in all the four cancer cell lines (Figure 4A).

Characteristics of the genes with the dual modification and the resultant gene silencing were then examined. To this end, from the genes with the dual modification, we isolated genes that had neither DNA methylation nor H3K27me3 and were expressed in normal counterpart cells (Supplementary Table 9 is available at *Carcinogenesis* Online). This group of genes, except for *SLC6A12* (in MCF7) and *SPSB4* (in MDA-MB-231), was repressed to almost undetectable levels in cancer cell lines (Figure 4B). Well-established tumor-suppressor genes, such as *IGFBP7* and *SFRP1*, were present among this group of genes. These results showed that the dual modification was involved in the repression of genes expressed in normal cells, including tumor-suppressor genes.

Efficient re-expression by combination of DNA demethylation and EZH2 inhibition

Re-expression of genes with the dual modification by a combined treatment with a DNA demethylating agent, 5-aza-dC and an EZH2 inhibitor, GSK126, was attempted (Figure 5A). Genes with the dual modification, such as *IGFBP7*, *SFRP1* and *SLC6A15*, were re-expressed more efficiently by the combined treatment than by a single treatment with 5-aza-dC or GSK126 (Figure 5B and C; Supplementary Figure 5 is available at *Carcinogenesis* Online). In contrast, the effect of combined treatment was not observed

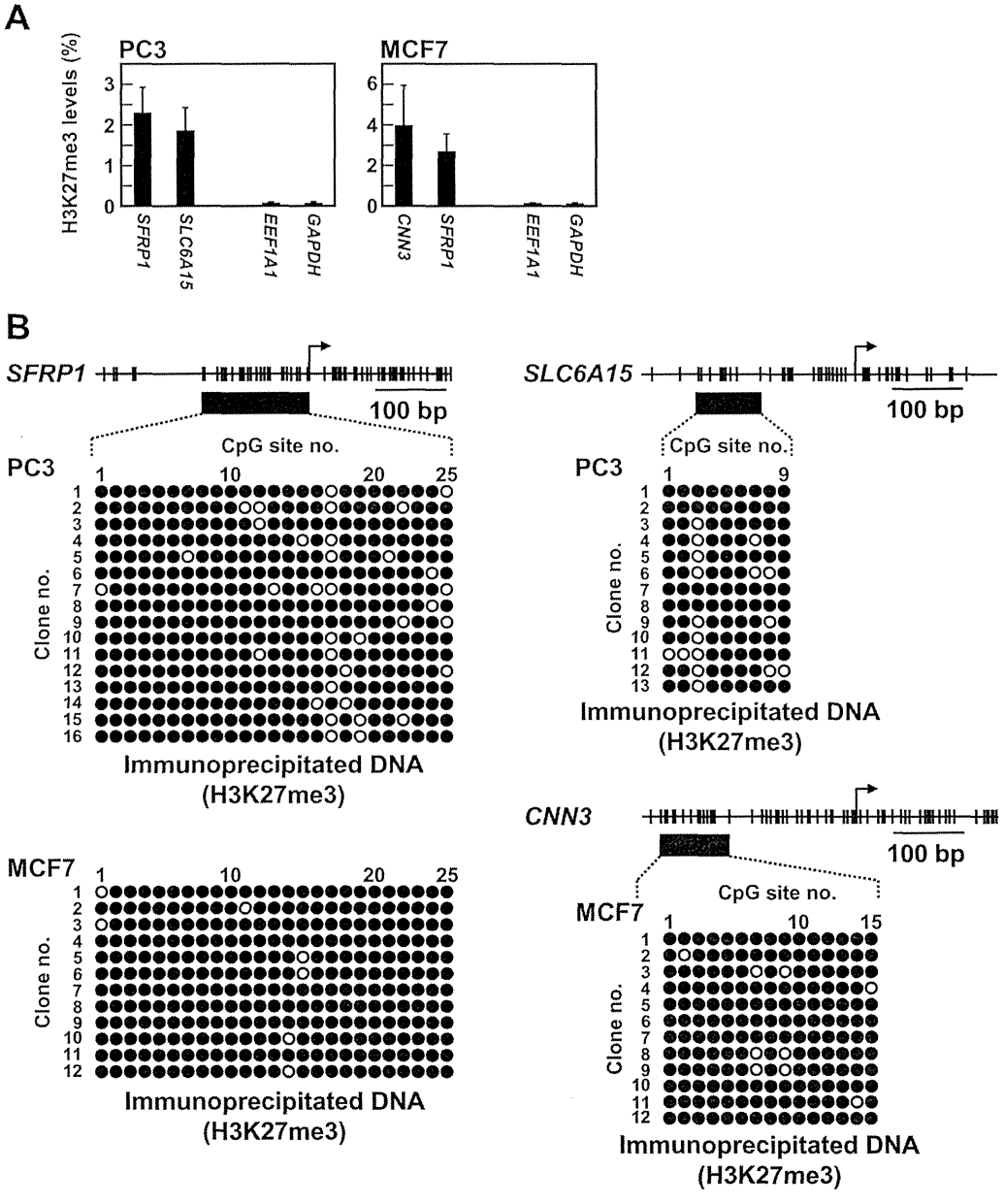

Figure 2. The coexistence of DNA methylation and H3K27me3 on the same DNA molecules. (**A**) H3K27me3 levels of genes with the dual modification. H3K27me3 levels were higher in the genes with the dual modification, *SFRP1*, *SLC6A15* and *CNN3*, than in housekeeping genes, *EEF1A1* and *GAPDH*. (**B**) Bisulfite sequencing of DNA molecules immunoprecipitated by anti-H3K27me3 antibody. All the DNA molecules were densely methylated for SFRP1 (PC3 and MCF7), SLC6A15 (PC3) and CNN3 (MCF7). Closed circle, methylated CpG site; open circle, unmethylated CpG site; vertical bar, CpG site; and arrow, TSS.

for genes with only DNA methylation (Figure 5B; Supplementary Figure 6 is available at *Carcinogenesis* Online) and genes with only H3K27me3 (Figure 5C; Supplementary Figure 7 is available at *Carcinogenesis* Online). Then, re-expression was confirmed in a genome-wide manner. Genes with the dual modification were re-expressed more efficiently by the combined treatment (Supplementary Figure 8 is available at *Carcinogenesis* Online). At the same time, even among the genes that had neither DNA methylation nor H3K27me3, 2-fold or more of upregulation was also observed (nonspecific changes) (Supplementary Figure 9 is available at *Carcinogenesis* Online).

The decrease of H3K27me3 level by a single treatment with GSK126 or by the combined treatment was confirmed in PC3 and MCF7 cell lines (Figure 5D–F; Supplementary Figure 2A is available at *Carcinogenesis* Online), but the EZH2 level was not changed (Figure 5E and F). These results showed that the combined treatment with a DNA demethylating agent and an EZH2 inhibitor was useful for re-expression of genes with the dual modification.

Additive inhibitory effect of the combination on cancer cell growth

First, the effect of the combined treatment with 5-aza-dC and GSK126 on growth of two cancer cell lines, PC3 and MCF7, was analyzed *in vitro* (Figure 6A and B). A single treatment with 5-aza-dC decreased growth of PC3 and MCF7 to 29.9 and 65.6%,

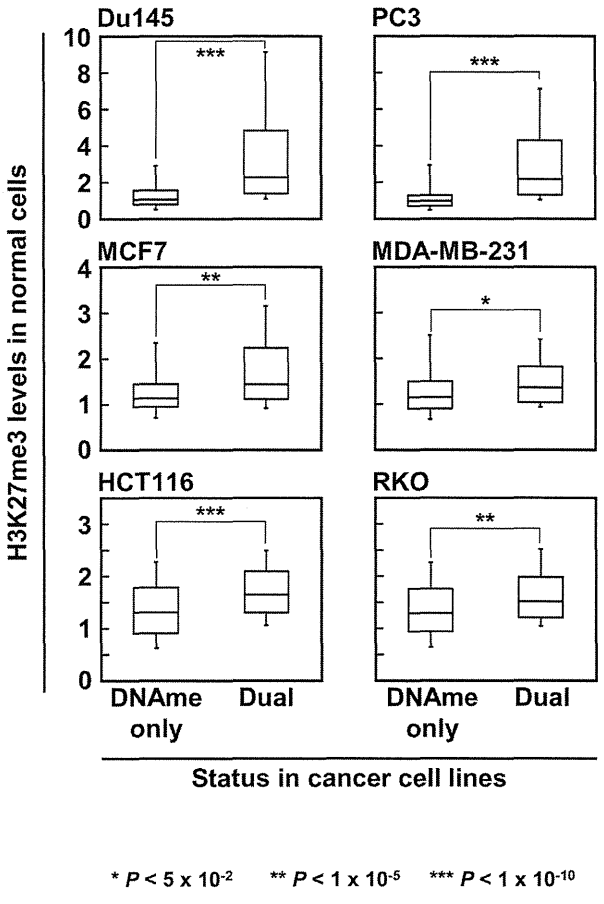

Figure 3. High H3K27me3 levels in normal cells of genes with the dual modification in cancer cells. H3K27me3 levels in normal cells were analyzed for genes with the dual modification and those with only DNA methylation in cancer cells. Genes with the dual modification had significantly higher levels of H3K27me3 than genes with only DNA methylation. The significance of difference was evaluated by the Mann–Whitney *U*-test ($^{*}P \leq 5 \times 10^{-2}$, $^{**}P \leq 1 \times 10^{-5}$, $^{***}P \leq 1 \times 10^{-10}$).

respectively, of untreated cells. A single treatment with GSK126 also decreased growth of PC3 and MCF7 to 76.7 and 42.9%, respectively, of untreated cells. The combined treatment with 5-aza-dC and GSK126 decreased growth of PC3 and MCF7 to 20.3 and 24.8%, respectively, of untreated cells.

Then, to compare these inhibitory effects with the combined treatment whose therapeutic efficacy was shown in a clinical trial (9), the effect of the combined treatment with 5-aza-dC and HDAC inhibitor, entinostat, was also analyzed (Supplementary Figure 10 is available at *Carcinogenesis* Online). A single treatment with entinostat decreased growth of PC3 and MCF7 to 66.9 and 42.7%, respectively, of untreated cells. The combined treatment with 5-aza-dC and entinostat decreased growth of PC3 and MCF7 to 18.5 and 30.8%, respectively, of untreated cells. These results showed that the combined treatment with a DNA demethylating agent and an EZH2 inhibitor had the additive inhibitory effect on growth of cancer cells, and the efficacy was comparable with that by the combined treatment with 5-aza-dC and entinostat.

Inhibitory effect of the combination on xenograft tumors

The effect of the combined treatment with 5-aza-dC and GSK126 on growth of PC3 xenograft tumors was analyzed. The combined treatment with 5-aza-dC and GSK126 inhibited growth of xenograft tumors (Figure 6C–E). In contrast, a single treatment with GSK126 had no inhibitory effect on growth of xenograft tumors, and that with 5-aza-dC could inhibit growth of six of eight xenografts. As for the side effects of the combined treatment, we did not observe significant changes of weights (Supplementary Figure 11A is available at *Carcinogenesis* Online). However, we observed a decrease in the numbers of leukocytes and erythrocytes and an increase in the number of platelets. The degree of these side effects was similar to those by a single treatment with 5-aza-dC (Supplementary Figure 11B is available at *Carcinogenesis* Online). These results showed that the combined treatment with 5-aza-dC and GSK126 inhibited growth of xenograft tumors more efficiently than a single treatment with 5-aza-dC.

Discussion

The combination of DNA demethylation and EZH2 inhibition had an additive inhibitory effect on cancer cell growth *in vitro*, and the efficacy was comparable with that by the combined treatment with 5-aza-dC and entinostat. The combined treatment also inhibited growth of xenograft tumors more efficiently than a single treatment with 5-aza-dC. This suggested that the cancer cell-specific dual modification is a promising target for cancer cell-specific epigenetic therapy. The effect of the combined treatment can be enhanced by (i) selecting DNA demethylating agents and EZH2 inhibitors suitable for combined treatment and (ii) optimizing the drug concentrations for the combination. Further to the increasing specificity for the dual modification, its reader proteins, if any, are ideal targets. The strategy of targeting a reader protein itself has been successful for histone acetylation, using inhibitors such as JQ1 and RVX-208, and was demonstrated to be effective in preclinical studies (42,43). Therefore, once reader proteins of the dual modification are identified, it might be possible to develop cancer cell-specific epigenetic therapy.

The presence of various physiological dual modifications, such as a combination of H3K4me3 and H3K27me3 (bivalent modification), has been reported (44). In this study, a cancer cell-specific combination of DNA methylation and H3K27me3 was used as a potential target for cancer cell-specific epigenetic therapy. However, genes with DNA methylation and H3K27me3 were also observed in normal cells although their number was extremely small, compared with that in cancer cells. In cancer cells, various epigenetic modifiers, such as DOT1L and EP300, are known to be dysregulated and their target modifications are altered (45,46). Therefore, the comparison of combinations of these epigenetic modifications between cancer cells and their normal counterpart cells might lead to identification of more combinations with cancer cell specificity.

Several known tumor-suppressor genes, such as *IGFBP7* and *SFRP1* (38–40), were among the genes with the dual modification. *IGFBP7* is known to be involved in the inhibition of the BRAF-MEK-ERK signaling pathway and also in the induction of cellular senescence and apoptosis (40). Repression of *IGFBP7* is critical for development of melanoma with BRAF V600E mutation (40). *SFRP1* is known as a negative regulator of the WNT signaling pathway, and repression of *SFRP1* leads to the activation of the WNT signaling pathway (47,48). The combination of DNA demethylation and EZH2 inhibition could induce re-expression of these genes. In addition to such an epigenetic effect, it is

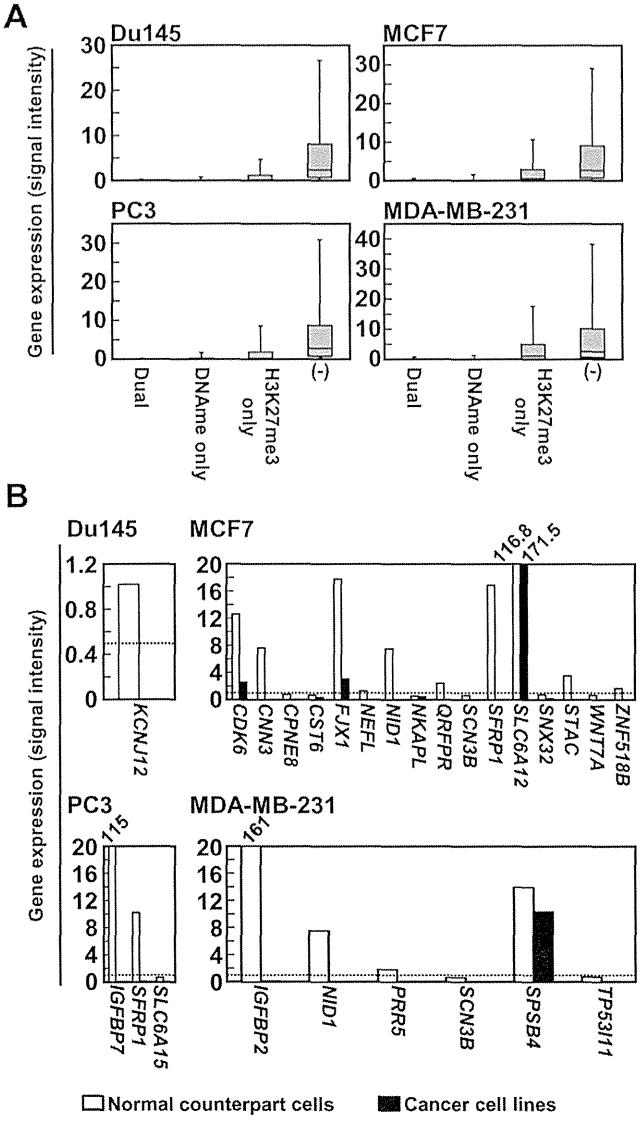

Figure 4. Repressive effect of the dual modification on gene expression. (A) Comparison of expression levels among four groups of genes–genes with the dual modification, those with only DNA methylation, those with only H3K27me3 and those without either. The genes with the dual modification had the lowest expression levels, along with those with only DNA methylation. (B) Repression of genes expressed in normal cells by the dual modification. From the genes with the dual modification, genes that had neither DNA methylation nor H3K27me3 and were expressed in normal counterpart cells were isolated. Expression levels were compared between cancer cell lines (black) and normal cells (white). Most of these genes were repressed to almost undetectable levels in cancer cell lines.

known that treatment with GSK126 induces both cytostatic and cytotoxic responses in lymphoma cell lines (13). Therefore, the therapeutic effect of the combined treatment was considered to be not only through the epigenetic effect but also through cytostatic and cytotoxic responses.

Mechanistically, in embryonic stem cells and normal cells, DNA methylation and H3K27me3 exist in a mutually exclusive manner (32,33). This is considered to be due to the inhibitory effect of DNA methylation on PRC2 recruitment (49). In contrast, in immortalized and transformed cells, the inhibitory effect of DNA methylation on PRC2 recruitment is known to be disrupted (33), and such disruption during carcinogenesis might be a possible mechanism of the preferential existence of the dual modification in cancer cells.

SLC6A12 and *SPSB4* were not repressed by the dual modification in cancer cells. As for the possible reasons, these genes might have been transcribed from TSSs different from the TSSs that had the dual modification. TSSs of a gene can vary from tissue to tissue depending upon genes (50), and a TSS in the database is not always accurate. It was also considered that only one allele of the gene had the dual modification in cancer cells and that the other allele was transcribed.

Combined treatment with 5-aza-dC and GSK126 induced marked re-expression of some genes with the dual modification, such as *CNN3*, *IGFBP7*, *NID1* and *SFRP1*, while not for the other genes, such as *CPNE8*, *NEFL* and *QRFPR*. To induce gene expression after the removal of repressive modifications, the presence of transcription factors required for the expression of individual genes is important. Therefore, it was considered that re-expression by the combined treatment might be dependent on the presence of sufficient amounts of such transcription factors in an analyzed cancer cell line.

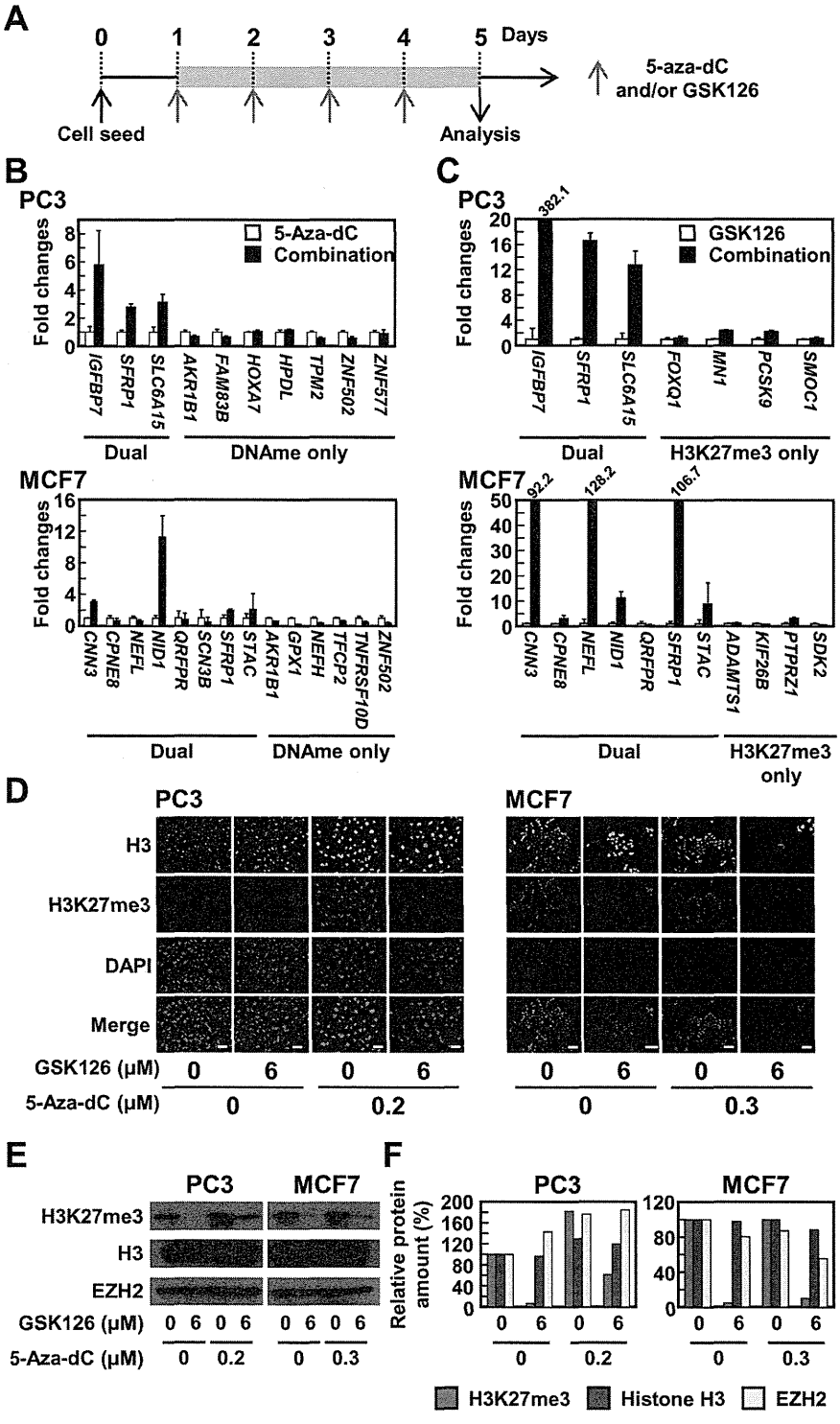

Figure 5. Efficient re-expression of genes with the dual modification by combination of DNA demethylation and EZH2 inhibition. (**A**) Experimental protocol of drug treatment. Two cancer cell lines, PC3 and MCF7, were treated with 5-aza-dC (0.2 μM for PC3 and 0.3 μM for MCF7) and/or GSK126 (6 μM) for 4 days, and harvested on day 5. (**B**), (**C**) Relative re-expression levels of genes with the dual modification and those with a single modification. The expression level of a gene in cells treated with the combination was normalized to that in cells treated with 5-aza-dC only (**B**) or to that in cells treated with GSK126 only (**C**). Genes with the dual modification were re-expressed more efficiently by the combined treatment than by a single treatment. (**D**) Immunofluorescence analysis of H3K27me3 in cells treated with 5-aza-dC and/or GSK126. The H3K27me3 level was decreased by a single treatment with GSK126 or by combined treatment with 5-aza-dC and GSK126. The scale bar represents 50 μm. (**E**), (**F**) Western blotting of H3K27me3 and EZH2 in cells treated with 5-aza-dC and/or GSK126. H3K27me3 levels were decreased by a single treatment with GSK126 and the combined treatment to 4.5–61.5% of those in untreated cells. EZH2 levels were not decreased by treatment with GSK126 as reported previously (13).

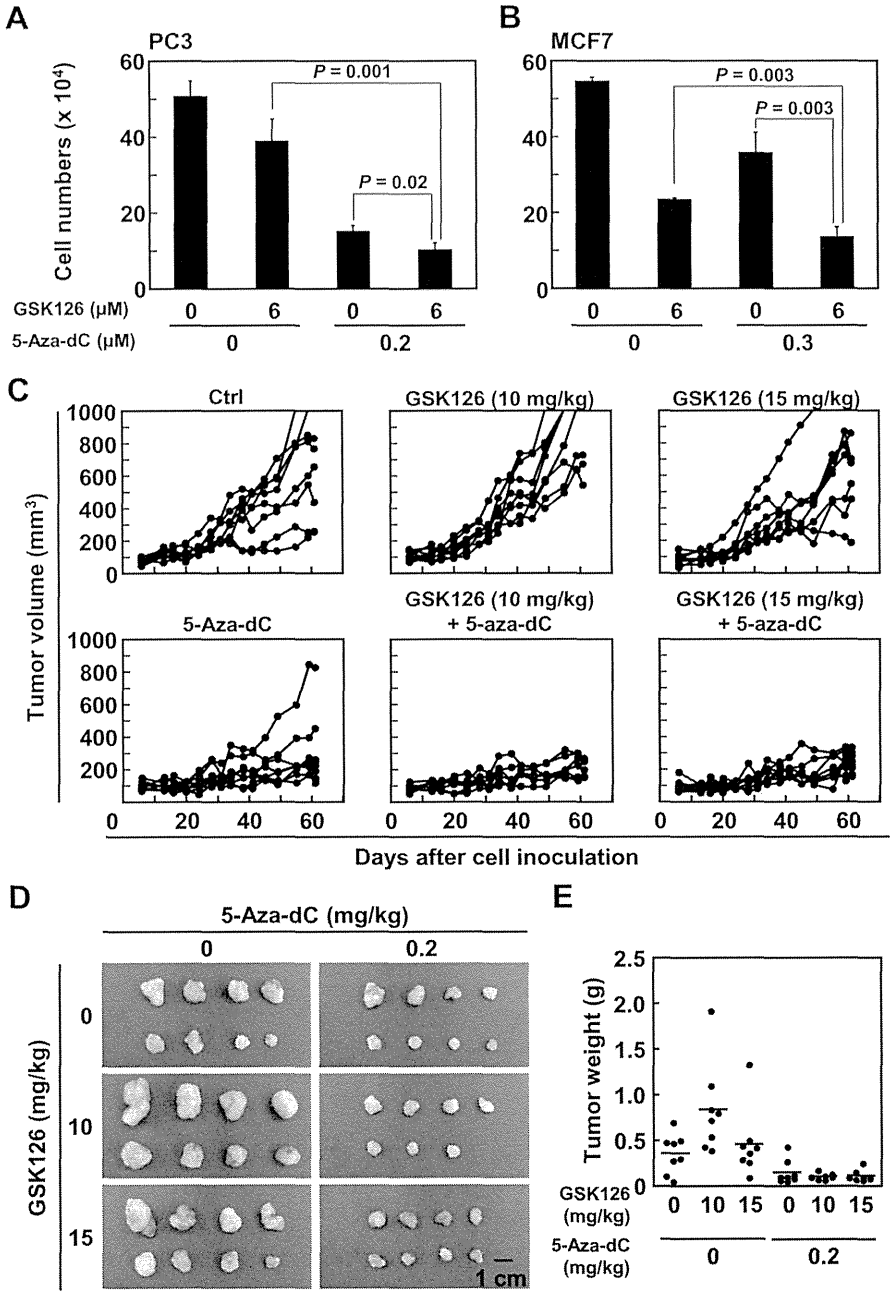

Figure 6. Therapeutic effects of the combination of DNA demethylation and EZH2 inhibition. (**A**), (**B**) Additive inhibitory effect of the combined treatment on cancer cell growth *in vitro*. Two cancer cell lines, PC3 and MCF7, were treated with the drugs according to the protocol shown in Figure 5A, and the cell number was counted on day 5. Additive inhibitory effect of the combination of DNA demethylation and EZH2 inhibition on cancer cell growth was observed in both PC3 (**A**) and MCF7 (**B**). The significance of difference was evaluated by the Student's t-test. (**C**), (**D**) and (**E**) The *in vivo* effect of the combined treatment. The combined treatment with 5-aza-dC and GSK126 reduced volume (**C**, **D**) and weight (**E**) of PC3 xenograft tumors more efficiently than a single treatment with 5-aza-dC.

In conclusion, a combination of DNA methylation and H3K27me3, which exists specifically in cancer cells, was considered to be a promising target for cancer cell-specific epigenetic therapy.

Supplementary material

Supplementary Table 1–9 and Figures 1–11 can be found at http://carcin.oxfordjournals.org/

Funding

Third-Term Comprehensive Cancer Control Strategy (H22-002) and Applied Research for Innovative Treatment of Cancer (H26-106) from the Ministry of Health, Labour and Welfare, Japan; Foundation for Promotion of Cancer Research in Japan; The National Cancer Center Research and Development Fund (26-A-15).

Conflict of Interest Statement: None declared.

References

1. Jones, P.A. et al. (2007) The epigenomics of cancer. Cell, 128, 683–692.
2. Laird, P.W. et al. (1996) The role of DNA methylation in cancer genetic and epigenetics. Annu. Rev. Genet., 30, 441–464.
3. Issa, J.P. (2007) DNA methylation as a therapeutic target in cancer. Clin. Cancer Res., 13, 1634–1637.
4. Mund, C. et al. (2010) Epigenetic cancer therapy: Proof of concept and remaining challenges. Bioessays, 32, 949–957.
5. DeWoskin, V.A. et al. (2013) The epigenetics pipeline. Nat. Rev. Drug Discov., 12, 661–662.
6. Kantarjian, H. et al. (2006) Decitabine improves patient outcomes in myelodysplastic syndromes: results of a phase III randomized study. Cancer, 106, 1794–1803.
7. Silverman, L.R. et al. (2002) Randomized controlled trial of azacitidine in patients with the myelodysplastic syndrome: a study of the cancer and leukemia group B. J. Clin. Oncol., 20, 2429–2440.
8. New, M. et al. (2012) HDAC inhibitor-based therapies: can we interpret the code? Mol. Oncol., 6, 637–656.
9. Juergens, R.A. et al. (2011) Combination epigenetic therapy has efficacy in patients with refractory advanced non-small cell lung cancer. Cancer Discov., 1, 598–607.
10. Daigle, S.R. et al. (2011) Selective killing of mixed lineage leukemia cells by a potent small-molecule DOT1L inhibitor. Cancer Cell, 20, 53–65.
11. Knutson, S.K. et al. (2013) Durable tumor regression in genetically altered malignant rhabdoid tumors by inhibition of methyltransferase EZH2. Proc. Natl. Acad. Sci. USA, 110, 7922–7927.
12. Kubicek, S. et al. (2007) Reversal of H3K9me2 by a small-molecule inhibitor for the G9a histone methyltransferase. Mol. Cell, 25, 473–481.
13. McCabe, M.T. et al. (2012) EZH2 inhibition as a therapeutic strategy for lymphoma with EZH2-activating mutations. Nature, 492, 108–112.
14. Qi, W. et al. (2012) Selective inhibition of Ezh2 by a small molecule inhibitor blocks tumor cells proliferation. Proc. Natl. Acad. Sci. USA, 109, 21360–21365.
15. Dammann, R. et al. (2000) Epigenetic inactivation of a RAS association domain family protein from the lung tumour suppressor locus 3p21.3. Nat. Genet., 25, 315–319.
16. Merlo, A. et al. (1995) 5' CpG island methylation is associated with transcriptional silencing of the tumour suppressor p16/CDKN2/MTS1 in human cancers. Nat. Med., 1, 686–692.
17. Rice, J.C. et al. (2000) Transcriptional repression of BRCA1 by aberrant cytosine methylation, histone hypoacetylation and chromatin condensation of the BRCA1 promoter. Nucleic Acids Res., 28, 3233–3239.
18. Fujii, S. et al. (2008) Enhancer of zeste homolog 2 downregulates E-cadherin by mediating histone H3 methylation in gastric cancer cells. Cancer Sci., 99, 738–746.
19. Osada, H. et al. (2008) Roles of achaete-scute homologue 1 in DKK1 and E-cadherin repression and neuroendocrine differentiation in lung cancer. Cancer Res., 68, 1647–1655.
20. Kondo, Y. et al. (2008) Gene silencing in cancer by histone H3 lysine 27 trimethylation independent of promoter DNA methylation. Nat. Genet., 40, 741–750.
21. Kouzarides, T. (2007) Chromatin modifications and their function. Cell, 128, 693–705.
22. Smith, Z.D. et al. (2013) DNA methylation: roles in mammalian development. Nat. Rev. Genet., 14, 204–220.
23. Di Croce, L. et al. (2013) Transcriptional regulation by Polycomb group proteins. Nat. Struct. Mol. Biol., 20, 1147–1155.
24. Levin, H.L. et al. (2011) Dynamic interactions between transposable elements and their hosts. Nat. Rev. Genet., 12, 615–627.
25. Hahn, M.A. et al. (2008) Methylation of polycomb target genes in intestinal cancer is mediated by inflammation. Cancer Res., 68, 10280–10289.
26. McCabe, M.T. et al. (2009) A multifactorial signature of DNA sequence and polycomb binding predicts aberrant CpG island methylation. Cancer Res., 69, 282–291.
27. Ohm, J.E. et al. (2007) A stem cell-like chromatin pattern may predispose tumor suppressor genes to DNA hypermethylation and heritable silencing. Nat. Genet., 39, 237–242.
28. Schlesinger, Y. et al. (2007) Polycomb-mediated methylation on Lys27 of histone H3 pre-marks genes for de novo methylation in cancer. Nat. Genet., 39, 232–236.
29. Takeshima, H. et al. (2009) The presence of RNA polymerase II, active or stalled, predicts epigenetic fate of promoter CpG islands. Genome Res., 19, 1974–1982.
30. Widschwendter, M. et al. (2007) Epigenetic stem cell signature in cancer. Nat. Genet., 39, 157–158.
31. Gal-Yam, E.N. et al. (2008) Frequent switching of Polycomb repressive marks and DNA hypermethylation in the PC3 prostate cancer cell line. Proc. Natl. Acad. Sci. USA, 105, 12979–12984.
32. Brinkman, A.B. et al. (2012) Sequential ChIP-bisulfite sequencing enables direct genome-scale investigation of chromatin and DNA methylation cross-talk. Genome Res., 22, 1128–1138.
33. Murphy, P.J. et al. (2013) Single-molecule analysis of combinatorial epigenomic states in normal and tumor cells. Proc. Natl. Acad. Sci. USA, 110, 7772–7777.
34. Gao, F. et al. (2014) Direct ChIP-bisulfite sequencing reveals a role of H3K27me3 mediating aberrant hypermethylation of promoter CpG islands in cancer cells. Genomics, 103, 204–210.
35. Kim, J.G. et al. (2013) Comprehensive DNA methylation and extensive mutation analyses reveal an association between the CpG island methylator phenotype and oncogenic mutations in gastric cancers. Cancer Lett., 330, 33–40.
36. Dennis, G. Jr et al. (2003) DAVID: Database for Annotation, Visualization, and Integrated Discovery. Genome Biol., 4, P3.
37. Huang da, W. et al. (2009) Systematic and integrative analysis of large gene lists using DAVID bioinformatics resources. Nat. Protoc., 4, 44–57.
38. Suzuki, H. et al. (2002) A genomic screen for genes upregulated by demethylation and histone deacetylase inhibition in human colorectal cancer. Nat. Genet., 31, 141–149.
39. Ugolini, F. et al. (2001) WNT pathway and mammary carcinogenesis: loss of expression of candidate tumor suppressor gene SFRP1 in most invasive carcinomas except of the medullary type. Oncogene, 20, 5810–5817.
40. Wajapeyee, N. et al. (2008) Oncogenic BRAF induces senescence and apoptosis through pathways mediated by the secreted protein IGFBP7. Cell, 132, 363–374.
41. Statham, A.L. et al. (2012) Bisulfite sequencing of chromatin immunoprecipitated DNA (BisChIP-seq) directly informs methylation status of histone-modified DNA. Genome Res., 22, 1120–1127.
42. Filippakopoulos, P. et al. (2010) Selective inhibition of BET bromodomains. Nature, 468, 1067–1073.
43. Picaud, S. et al. (2013) RVX-208, an inhibitor of BET transcriptional regulators with selectivity for the second bromodomain. Proc. Natl. Acad. Sci. USA, 110, 19754–19759.
44. Bernstein, B.E. et al. (2006) A bivalent chromatin structure marks key developmental genes in embryonic stem cells. Cell, 125, 315–326.
45. Füllgrabe, J. et al. (2011) Histone onco-modifications. Oncogene, 30, 3391–3403.
46. Plass, C. et al. (2013) Mutations in regulators of the epigenome and their connections to global chromatin patterns in cancer. Nat. Rev. Genet., 14, 765–780.
47. Jones, S.E. et al. (2002) Secreted Frizzled-related proteins: searching for relationships and patterns. Bioessays, 24, 811–820.
48. Nojima, M. et al. (2007) Frequent epigenetic inactivation of SFRP genes and constitutive activation of Wnt signaling in gastric cancer. Oncogene, 26, 4699–4713.
49. Bartke, T. et al. (2010) Nucleosome-interacting proteins regulated by DNA and histone methylation. Cell, 143, 470–484.
50. Carninci, P. et al. (2006) Genome-wide analysis of mammalian promoter architecture and evolution. Nat. Genet., 38, 626–635.

J Cancer Res Clin Oncol (2015) 141:453–463
DOI 10.1007/s00432-014-1841-x

ORIGINAL ARTICLE – CANCER RESEARCH

ZNF695 methylation predicts a response of esophageal squamous cell carcinoma to definitive chemoradiotherapy

Takamasa Takahashi · Satoshi Yamahsita · Yasunori Matsuda · Takayoshi Kishino · Takeshi Nakajima · Ryoji Kushima · Ken Kato · Hiroyasu Igaki · Yuji Tachimori · Harushi Osugi · Masato Nagino · Toshikazu Ushijima

Received: 24 June 2014 / Accepted: 20 September 2014 / Published online: 2 October 2014

Abstract
Purpose Definitive chemoradiotherapy (dCRT) is one of the standard treatments for esophageal squamous cell carcinoma. Patients with a response to dCRT have a better prognosis than those resistant to dCRT while survival benefits for patients with residual tumors are limited. Nevertheless, few molecular markers to predict the response to dCRT are currently available. Here, we aimed to establish a DNA methylation marker to predict the response to dCRT.
Methods A total of 104 patients were divided into screening ($n = 43$) and validation ($n = 61$) sets. A genome-wide DNA methylation analysis was performed using an Infinium HumanMethylation450 BeadChip array. Methylation levels were measured by quantitative methylation-specific PCR and normalized by the fraction of cancer cells in a sample.
Results The genome-wide methylation analysis of seven responders and eight non-responders identified 18 genomic regions specifically (un)methylated in the responders. Among these, methylation of the promoter CpG island of *ZNF695* was significantly associated with the response to dCRT in the screening set ($P = 0.004$), and a cutoff value was determined. In the validation set, the association was successfully validated ($P = 0.021$), and a high specificity (90 %) for the prediction of responders was obtained using the prefixed cutoff value. In addition, a multivariate analysis showed that *ZNF695* methylation was an independent predictive factor for the response to dCRT (OR 7.55, 95 % CI 2.12–26.9, $P = 0.002$).
Conclusion *ZNF695* methylation was significantly associated with the response to dCRT and is a promising predictive marker for the response to dCRT.

Keywords Epigenetics · DNA methylation · Biomarker · Esophageal squamous cell carcinoma · Chemoradiotherapy

Electronic supplementary material The online version of this article (doi:10.1007/s00432-014-1841-x) contains supplementary material, which is available to authorized users.

T. Takahashi · S. Yamahsita · Y. Matsuda · T. Kishino · T. Ushijima (✉)
Division of Epigenomics, National Cancer Center Research Institute, 5-1-1 Tsukiji, Chuo-ku, Tokyo 104-0045, Japan
e-mail: tushijim@ncc.go.jp

T. Takahashi · T. Kishino · H. Igaki · Y. Tachimori
Esophageal Surgery Division, National Cancer Center Hospital, Tokyo, Japan

T. Takahashi · M. Nagino
Division of Surgical Oncology, Department of Surgery, Nagoya University Graduate School of Medicine, Nagoya, Japan

Y. Matsuda · H. Osugi
Department of Gastroenterological Surgery, Graduate School of Medicine, Osaka City University, Osaka, Japan

T. Nakajima
Endoscopy Division, National Cancer Center Hospital, Tokyo, Japan

R. Kushima
Pathology and Clinical Laboratory Division, National Cancer Center Hospital, Tokyo, Japan

K. Kato
Gastrointestinal Medical Oncology Division, National Cancer Center Hospital, Tokyo, Japan

Introduction

Esophageal squamous cell carcinoma (ESCC) is a predominant histological type of esophageal cancer worldwide and one of the most serious malignant cancers due to its rapid development and fatal prognosis (Chung et al. 2010; Pennathur et al. 2013). The prognosis of patients with advanced ESCC is still unsatisfactory although aggressive treatment strategies, such as surgery with preoperative or postoperative chemotherapy or preoperative chemoradiotherapy (CRT), and definitive CRT (dCRT) (Allum et al. 2009; Ando et al. 2003, 2012; Blum et al. 2013; Conroy et al. 2014; Kato et al. 2011, 2013; Kelsen et al. 2007; Kleinberg and Forastiere 2007; Tepper et al. 2008; van Hagen et al. 2012), have been implemented. Among these aggressive treatments, dCRT has been an important therapeutic strategy for advanced ESCC (Conroy et al. 2014; Kato et al. 2011, 2013; Kleinberg and Forastiere 2007; van Hagen et al. 2012). By dCRT, a complete response of primary tumor is seen in 58.0–70.6 % of patients (Kato et al. 2011, 2013; Tahara et al. 2005), and such patients not only have a good prognosis but also can preserve their esophagus and keep a better quality of life than patients who undergo esophagectomy. In contrast, survival benefits of dCRT for patients who have residual tumors are limited even after adequate salvage treatments (Conroy et al. 2014; Kato et al. 2011, 2013). Although preoperative chemo- or chemoradiotherapy followed by surgery may be powerful, operative mortality and morbidity are not ignored. If we can predict the response of ESCC to dCRT before starting a treatment, we can stratify patients who will benefit by it for personalized treatments.

To establish a biomarker to predict the response of ESCC to dCRT, a lot of effort has been made in the field of molecular markers, and markers using specific RNA and protein expression have been reported (Akutsu et al. 2011; Gao et al. 2013; Makuuchi et al. 2013; Okamoto et al. 2013; Zhang et al. 2013). Although these markers were associated with the response to dCRT, their utility has not been confirmed by independent studies yet. Also, their accuracy even in the screening set was not satisfactory for clinical use. Therefore, further searching for a predictive marker for dCRT is required, and validating the utility of the marker is essential for clinical application.

As a molecular marker, DNA methylation has several advantages over RNA and proteins (Goel 2010; Issa 2012; Laird 2003). First, DNA methylation status is stable, even if a cell is placed in different environments, and consistent results can be obtained even under different conditions of sample collection where gene expression profiles are affected. Secondly, DNA methylation can be analyzed using DNA, which can remain relatively intact in samples with RNA and protein degradation. Thirdly, DNA methylation has only two statuses, methylated or unmethylated, and its profile cannot be affected by a small amount of contaminating cells, different from gene expression. Also, DNA methylation status has been reported to correlate with clinicopathological features of many types of cancers (Brait et al. 2008; Kim et al. 2013; Sato et al. 2002; Yang and Park 2012). Taking these advantages, DNA methylation markers for the prediction of a response to a cancer therapy have been identified in other types of cancers (Amatu et al. 2013; Giovannetti et al. 2012; Hegi et al. 2005; Mikeska et al. 2012; Park et al. 2009; Toyota et al. 2009). However, in ESCC, few studies have demonstrated an association between DNA methylation status and response to dCRT (Brabender et al. 2009).

In the present study, we aimed to identify genomic regions whose methylation statuses are associated with the response of ESCC to dCRT by a genome-wide methylation analysis and to validate the isolated candidate predictive markers for the response to dCRT.

Methods

Samples and patient profiles

A total of 187 ESCC samples were collected from ESCC patients from January 2006 to April 2013 at the National Cancer Center Hospital and the Osaka City University Hospital. This study was approved by the Institutional Review Board of the National Cancer Center, Tokyo, Japan (Reference No. 2010-094), and the Osaka City University, Osaka, Japan (Reference No. 1500). Written informed consents were obtained from all the individuals. They had histologically confirmed ESCC and were at cStage II–IV according to the 6th edition of the TNM classification (Sobin 2002). Patients with clinical T4 and with distant organ metastasis were excluded.

A group of 128 patients underwent chemotherapy comprised of two courses of infusion of 5-fluorouracil (5-FU) (700 mg/m^2/day) on days 1–4 and 29–32 and 2-h infusion of cisplatin (CDDP) (70 mg/m^2) on days 1 and 29. A total of 60 Gy was concurrently administered in 30 fractions. A 1-week break was provided after 30 Gy irradiation, and radiotherapy was resumed on day 29 with the second chemotherapy course. The other group of 59 patients underwent chemotherapy comprised of two courses of infusion of 5-FU (1,000 mg/m^2/day) on days 1–4 and 29–32 and a 2-h infusion of CDDP (75 mg/m^2) on day 1 and 29. A total of 50.4 Gy was concurrently administered in 28 fractions. Break period of radiation was not planned. An additional two cycles of chemotherapy were conducted after completion of the radiotherapy until the tumor disappeared or progressed.